

Prediction of Indian summer monsoon in short to medium range time scale with high resolution global forecast system (GFS) T574 and T382

V. R. Durai · S. K. Roy Bhowmik

Received: 6 November 2012/Accepted: 23 July 2013/Published online: 8 August 2013
© Springer-Verlag Berlin Heidelberg 2013

Abstract Performance of national centers for environmental prediction based global forecast system (GFS) T574/L64 and GFS T382/L64 over Indian region has been evaluated for the summer monsoon season of 2011. The real-time model outputs are generated daily at India Meteorological Department, New Delhi for the forecasts up to 7 days. Verification of rainfall forecasts has been carried out against observed rainfall analysis. Performance of the model is also examined in terms of lower tropospheric wind circulation, vertical structure of specific humidity and precipitable water content. Case study of a monsoon depression is also illustrated. Results obtained show that, in general, both the GFS T382 and T574 forecasts are skillful to capture climatologically heavy rainfall regions. However, the accuracy in prediction of location and magnitude of rainfall fluctuates considerably. The verification results, at the spatial scale of 50 km resolution, in a regional spatial scale and country as a whole, in terms of continuous skill score, time series and categorical statistics, have demonstrated superiority of GFS T574 against T382 over Indian region. Both the model shows bias of lower tropospheric drying and upper tropospheric moistening. A bias of anti-cyclonic circulation in the lower tropospheric level lay over the central India, where rainfall as well as precipitable water content shows negative bias. Considerable differences between GFS T574 and T382 are noticed in the structure of model bias in terms of lower tropospheric wind circulation, vertical structure of specific humidity and precipitable water contents. The magnitude of error for these parameters increases with forecast lead time in both GFS T574

and T382. The results documented are expected to be useful to the forecasters, monsoon researchers and modeling community.

Keywords GFS T382L64 · T574L64 · NWP · Global model · Rainfall analysis · QPE · Indian summer monsoon · Rainfall prediction skill

1 Introduction

The global forecast system GFS T382L64 (~ 35 km in horizontal over the tropics), adopted from national centers for environmental prediction (NCEP), was implemented at India meteorological department (IMD), New Delhi on IBM based high power computing systems (HPCS) in May 2010. Very recently in the year 2012, GFS T382 has been replaced by the upgraded version of the model GFS T574L64 (version *GSM 9.1.0*) (~ 25 km in horizontal over the tropics). During 2011, the T574 was being run in an experimental mode to assess its forecast skill, while the T382 was being run in an operational mode. Real-time forecast products of both the models were made available to the national web site of IMD (www.imd.gov.in).

Numerical weather prediction (NWP) model verification is an indispensable part of meteorological research and operational forecasting activities. If the verification methodology is properly designed, verification results can effectively meet the needs of many diverse groups, including modellers, forecasters, and users of forecast information. It can be used to direct research, to determine where research funding is most needed, to check that forecasts are improving with time, to help operational modelling centers for model upgrades. One of the most critical issues in modeling the global atmosphere and climate by general circulation models

V. R. Durai (✉) · S. K. Roy Bhowmik
India Meteorological Department, New Delhi 110003, India
e-mail: durai.imd@gmail.com

(GCMs) is the simulation and initialization of precipitation processes. Validation of Global NWP model determines the confidence related to a particular forecast over a specific region, but it can also be thought of as a preliminary evaluation of simulated climate drift that can be expected from the model being tested. This idea is further illustrated by Saulo et al. (2001) who validated the systematic errors of NCEP and LAHM Regional Model Daily Forecasts over Southern South America. Performance statistics for the precipitation forecast of many NWP models have been documented by various authors such as, McBride and Ebert (2000) and Doswell et al. (1990), etc.

The study of Yang et al. (2006) evaluates the performance of the NCEP Global Forecast System (GFS) against observations made by the US Department of Energy Atmospheric Radiation Measurement (ARM) Program at the southern Great Plains site for the years 2001–2004. Results show that the overall performance of the GFS model has been improving, although certain forecast errors remain. Rainfall is one of the most difficult parameters to predict due to its large spatial and temporal variation. Durai et al. (2010a), studied the rainfall prediction skill of NCEP GFS T254 over Indian region during summer monsoon 2008. A detailed rainfall prediction skill of the GFS model is described in this paper.

The main purpose of this study is to document the performance skill of GFS T574 against the performance skill of GFS T382, on the basis of daily day-1 to day-7 forecasts generated during summer monsoon 2011 (1 June to 30 September) over India in short to medium range time scale. Model performance is evaluated for day-1 to day-5 forecasts of 24-h accumulated and 7 days cumulative rainfall in terms of several accuracy and skill measures. Performance of the model is also examined in terms of lower tropospheric wind circulations, vertical structure of specific humidity and spatial distribution of precipitable water content (PWC) to understand the monsoon rainfall features captured by the model. The performance of the model during the episode of a monsoon depression is also illustrated in this study.

This paper comprises of five sections. Section 2 gives a brief description of NCEP GFS used at IMD. The verification procedures used in this work are described in Sect. 3. Results of verifications are presented in Sect. 4. Rainfall prediction skill and comparison of results are discussed in Sect. 4.1. Verification results of monsoon flow features and a case study of monsoon depression are presented in Sect. 4.2. Finally, the summary and concluding remarks are given in Sect. 5.

2 The NCEP GFS

The NCEP GFS run at IMD is a primitive equation spectral global model with state of art dynamics and physics

(Kanamitsu 1989; Kalnay et al. 1990; Kanamitsu et al. 1991; Moorthi et al. 2001). This GFS model is conforming to a dynamical framework known as the Earth System Modeling Framework (ESMF) and its code was restructured to have many options for updated dynamics and physics. The topographic map of India for GFS at T382 and T574 resolution is shown in Fig. 1a. Colour shading indicates the areas of terrain elevation (Fig. 1a) greater than 250 m above mean sea level. The inter-comparison reveals that peak terrain features are better represented in the T574. Details about the global forecast model (GFS) are available at <http://www.emc.ncep.noaa.gov/GFS/doc.php>. A brief introduction about model physics and dynamics options of GFS T382 and GFS T574 are discussed below.

The model physics changes from GFS T382 to GFS T574 were mainly in radiation, gravity wave drag, planetary boundary layer processes, shallow and deep convection schemes and an introduction of tracer transport scheme in the vertical (Saha et al. 2010). Long wave (LW) computation frequency was set as 1 h and added stratospheric aerosol and tropospheric aerosol (LW) in the rapid radiative transfer model (Mlawer et al. 1997). Aerosol single scattering albedo was set as 0.99. SW aerosol asymmetry factor was changed and the new aerosol climatology was used. SW cloud overlap was changed from random to maximum random overlap. Time varying global mean CO₂ was used instead of constant CO₂. Treatment of the dependence of direct-beam surface albedo on solar zenith angle over snow-free land surface is following Yang et al. (2008). Gravity wave drag (GWD) routine was also modified to automatically scale mountain block and GWD stress. Planetary boundary layer (PBL) processes included stratocumulus-top driven turbulence mixing, enhanced stratocumulus-top driven diffusion for cloud top entrainment instability and local diffusion for night time stable PBL. Background diffusion in inversion layers over ocean is reduced by 70 % to decrease the erosion of stratocumulus along the coastal area. Bulk-Richardson number is used to calculate PBL height.

Shallow convection is changed from old Tiedke's scheme to new mass-flux shallow convection scheme (Han and Pan 2010), which detrains cloud water from every updraft layer. Convection starting level is defined as the level of maximum moist static energy within PBL. Cloud top is limited to 700 hPa. Entrainment rate is given to be inversely proportional to height and detrainment ratio is set to be a constant as entrainment rate at the cloud base. Mass flux at the cloud base is given to be a function of convection boundary layer velocity scale. Deep convection parameterization follows modified Simplified-Arakawa-Scheme (Han and Pan 2006). It eliminates random cloud type, and detrains cloud water from every cloud layer of the height cloud. Finite entrainment and detrainment rates for heat, moisture and momentum are specified. Similar to

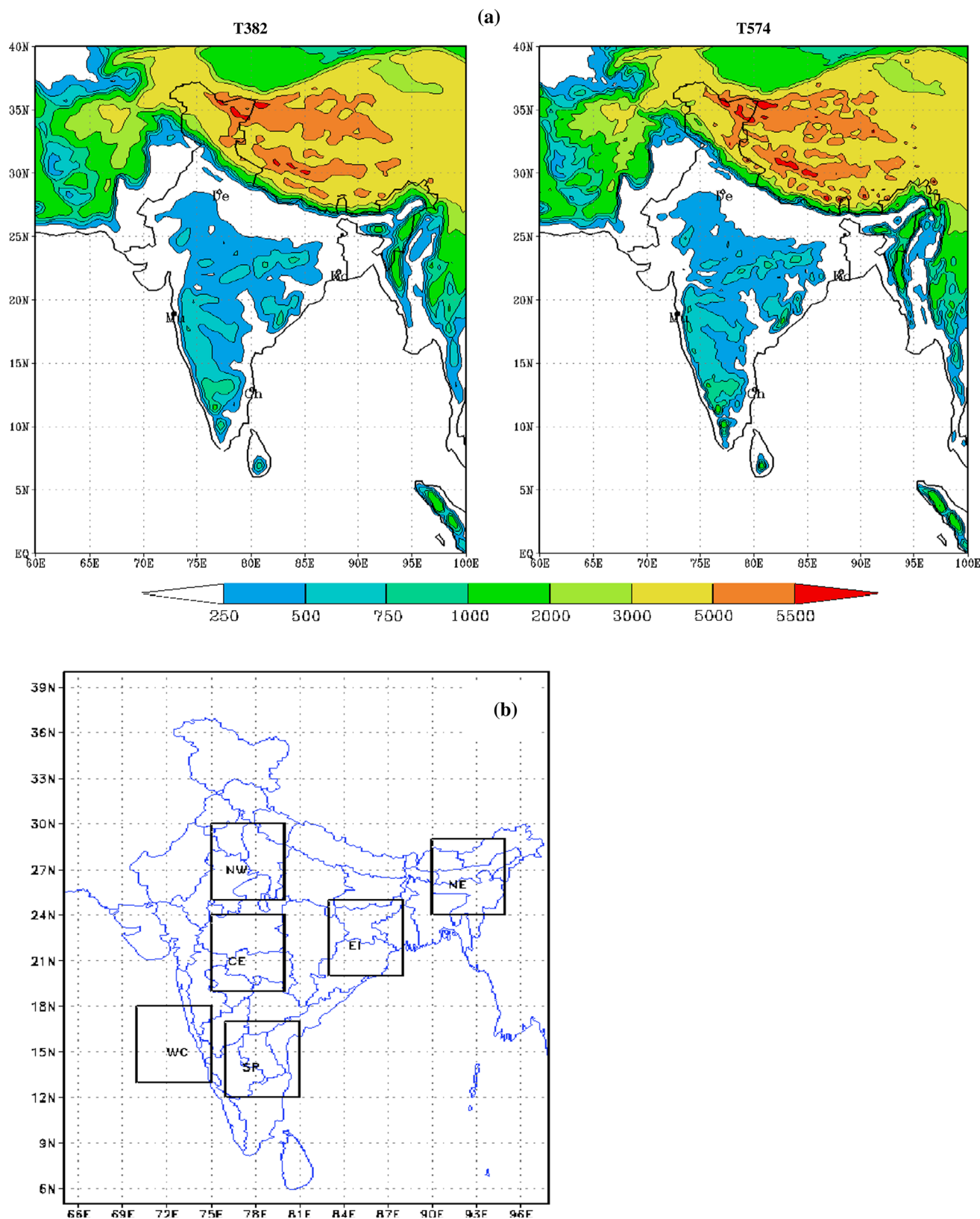


Fig. 1 **a** Topography of GFS T382 and GFS T574; Shading indicates areas of terrain elevation greater than 250 m above mean sea level, **b** the region of study: different regions are shown in outline:

NW, North West India; CE, Central India; EI, Eastern India; NE, North East India; WC, West Coast of India and SP, South Peninsula India

shallow convection scheme, entrainment rate is given to be inversely proportional to height in sub-cloud layers and detrainment rate is set to be a constant as entrainment rate at the cloud base. Above cloud base, an organized entrainment is added, which is a function of environmental relative humidity. Intra-seasonal momentum background diffusivity is applied for winds only. Convective overshooting increased cloud water detrainment in upper cloud layers.

The assimilation system (for GFS T574) is a global 3-dimensional variational technique, based on NCEP Grid Point Statistical Interpolation (GSI 3.0.0; Kleist et al. 2009) scheme, which is the next generation of Spectral Statistical Interpolation (SSI; David and Derber 1992). The major changes incorporated in T574 GDAS compared to T382 GDAS are: use of variational quality control, flow dependent re-weighting of background error statistics, use of new version of Community Radiative Transfer Model (CRTM 2.0.2), improved tropical cyclone relocation algorithm, changes in the land, snow and ice skin temperature and use of some new observations in the assimilation cycle. Details of data presently being processed for GFS at IMD are available at http://www.imd.gov.in/section/nhac/dynamic/data_coverage.pdf.

In the operational mode, the Global Data Assimilation System (GDAS) cycle runs 4 times a day (00 UTC, 06 UTC, 12 UTC and 18 UTC) and GFS model runs 2 times a day (00 and 12 UTC). The analysis and forecast for 7 days are performed using the High Power Computing System (HPCS) installed in IMD Delhi. One GDAS cycle and 7 days (day-1 to day-7) GFS forecast at T382L64 (~ 35 km in horizontal over the tropics) takes about 30 min on IBM Power 6 (P6) machine using 20 nodes with seven tasks (seven processors) per node, while the same for GFS T574 (~ 25 km in horizontal over the tropics) is approximately 1 h 40 min.

3 Data and methodology

3.1 Rainfall

In this study rainfall verifications were carried out for both the GFS T382 and GFS T574 model runs at 00 UTC against daily rainfall analysis at the resolution of 50 km based on the merged rainfall data combining gridded rain gauge observations prepared by IMD Pune for the land areas and TRMM 3B42RT data for the Sea areas (Durai et al. 2010b). Model performance is evaluated for day-1 to day-5 forecasts of 24-h accumulated precipitation over Indian monsoon region by computing and comparison of skill scores, such as: mean error, root mean square error and anomaly correlation coefficient

between forecast and analysis in spatial resolution of 50 km. For computation of anomaly Correlation Coefficient (CC), observed daily precipitation climatology on the basis of gridded daily rainfall dataset (Rajeevan et al. 2005) based on rain gauge measurements from 1803 stations over Indian land for the period 1951–2003 from IMD is used.

In order to examine the performance of the model in the regional spatial scale for different homogeneous regions of the country, we selected (Fig. 1b) seven representative region (square/rectangular domain) for (1) All India land areas: (Lon: 68°E–98°E, Lat: 9°N–37°N), (2) Central India (CE: Lon: 75°E–80°E, Lat: 19°N–24°N), covering Vidarbha and neighborhoods, (3) East India (EI: Lon: 75°E–80°E, Lat: 19°N–24°N), covering Orissa and neighborhoods, (4) North-east India (NE: Lon: 90°E–95°E, Lat: 24°N–29°N), (5) North-west India (NW: Lon: 75°E–80°E, Lat: 25°N–30°N), covering Rajasthan and Haryana, (6) South Peninsular India (SP: Lon: 76°E–81°E, Lat: 12°N–17°N), covering Kerala and neighborhood and (7) West coast of India (WC: Lon: 70°E–75°E, Lat: 13°N–18°N), covering Konkan–Goa. The domains mean values of weekly (0–168 h) cumulative rainfall forecast from both GFS T382 and T574 is compared against observation and, also the temporal and spatial correlation is computed.

In addition to these simple measures, a number of categorical statistics are applied. The term categorical refers to the yes/no nature of the forecast verification at each grid point. Some threshold (i.e., 0.1, 1, 2, 5, 10, 15, 35, 65 mm/day) is considered to define the transition between rain versus no-rain event. Then at each grid point (at the resolution of 50 km), each verification time is scored as falling under one of the four categories of correct no-rain forecasts (Z), false alarms (F), misses (M), or hits (H). A number of categorical statistical skill measures are used, computed from the elements of rain/no-rain contingency Table. They include

$$\text{Bias score (Bias)} : BS = \frac{F + H}{M + H}$$

$$\text{Probability of detection (POD)} : POD = \frac{H}{H + M}$$

$$\text{Threat score (TS)} : TS = \frac{H}{H + M + F}$$

$$\text{Equitable threat score (ETS)} : ETS = \frac{H - H_{\text{random}}}{H + M + F - H_{\text{random}}}$$

$$\text{where } H_{\text{random}} = \frac{(H + M)(H + F)}{\text{total}}$$

3.2 Monsoon circulation features

In order to understand the characteristic features of monsoon rainfall captured by the model, performance of the

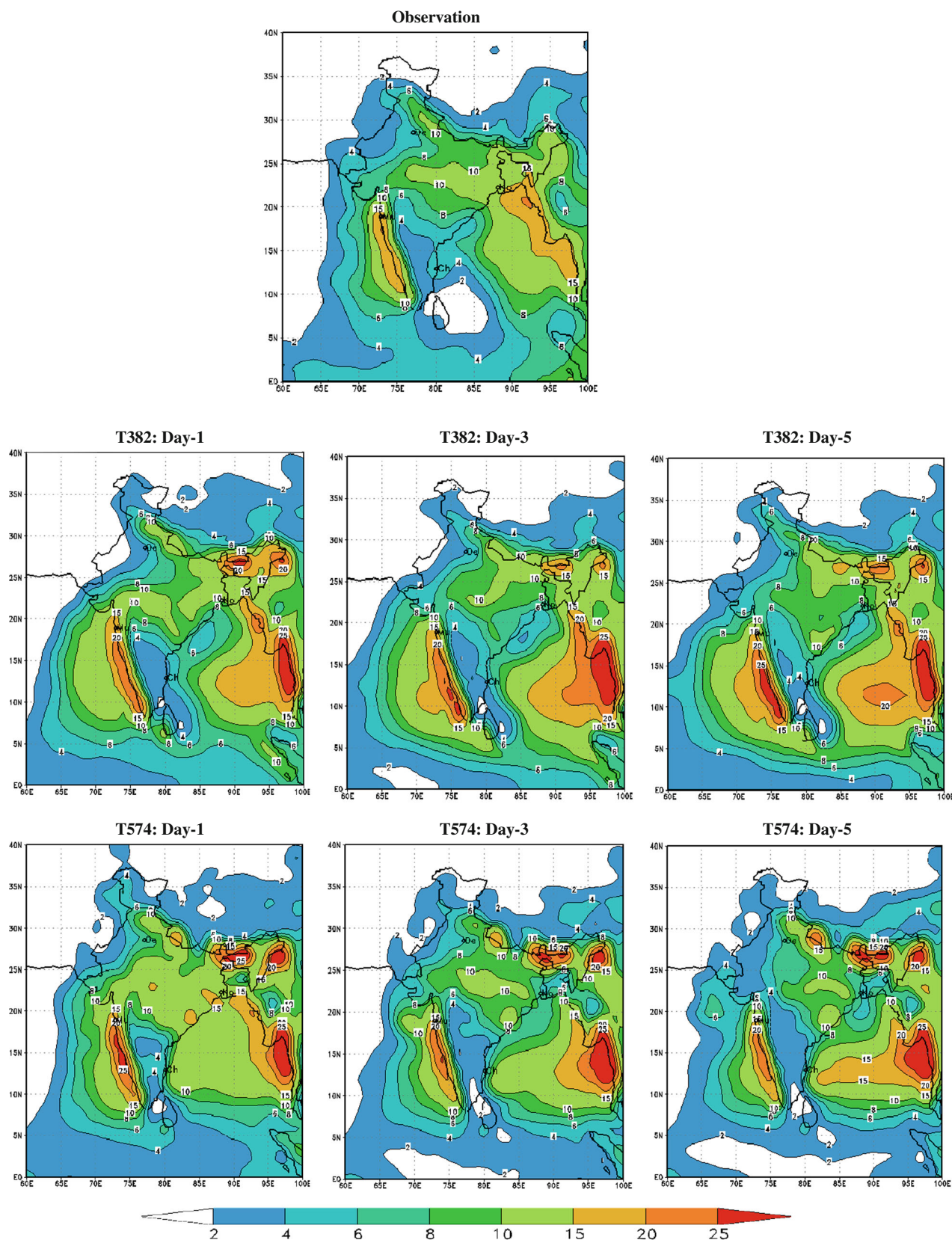


Fig. 2 Spatial distribution of seasonal mean observed rainfall (mm/day); and day-1, day-3 and day-5 forecasts from GFS T382 (top panel) and GFS T574 (bottom panel) for the period from 1 June to 30 September 2011

model is also examined in terms of lower tropospheric circulation, vertical structure of specific humidity and spatial distribution of precipitable water content (PWC). A case study of a monsoon depression is illustrated to examine the performance of the model during the episode of monsoon depression.

The PWC in an atmospheric column is given by:

$$PWC = \frac{1}{g} \int_{P_{sur}}^{P_{top}} q dp$$

where the limit of the integration is from the surface to the top (300 hPa) of the atmosphere up to which the value of specific humidity q is non-zero and g is the acceleration due to gravity.

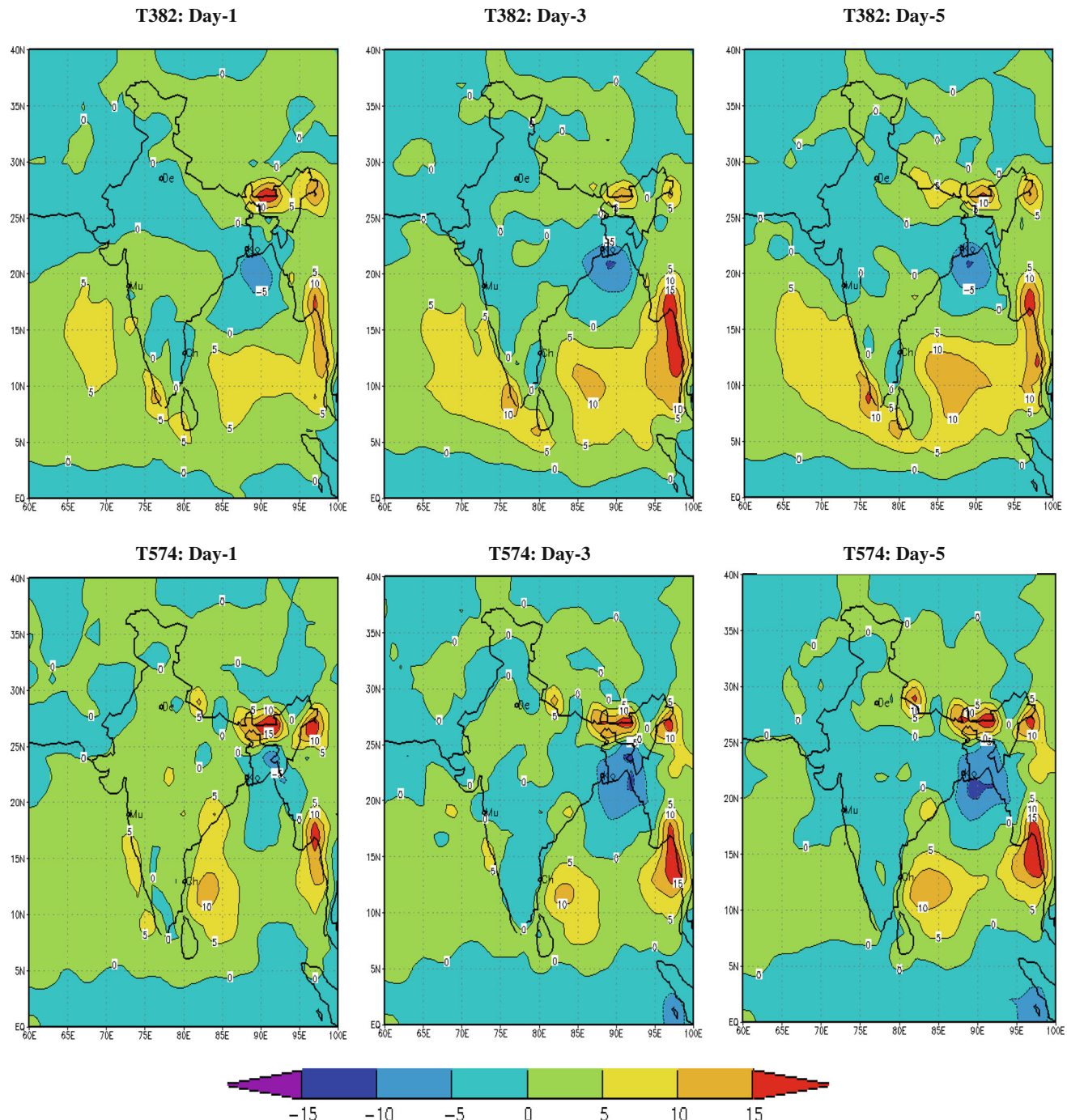


Fig. 3 Spatial distribution of seasonal mean error (forecast-observed) rainfall (mm/day) based on day-1, day-3 and day-5 forecasts of GFS T382 (top panel) and GFS T574 (bottom panel) for the period from 1 June to 30 September 2011

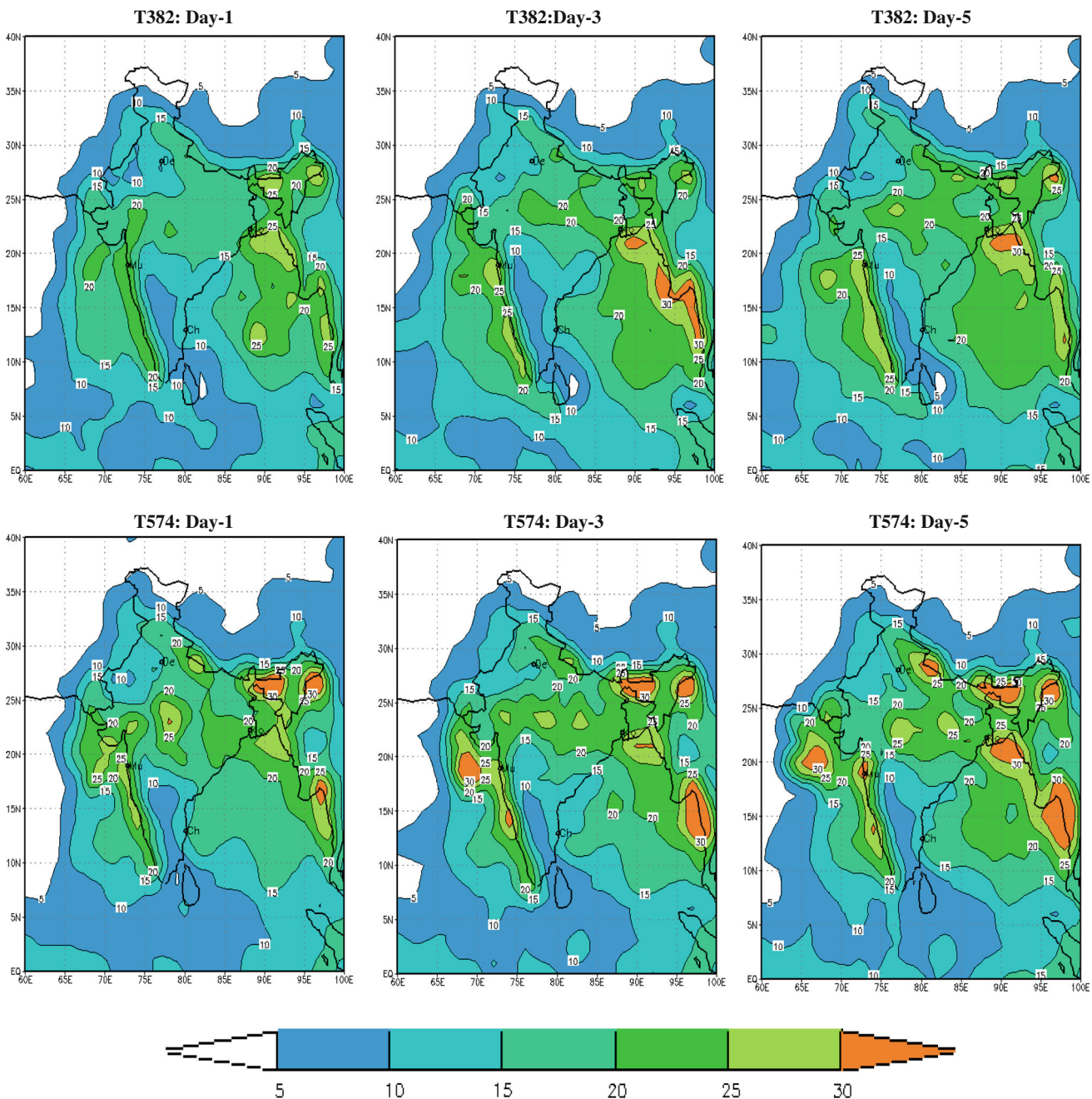


Fig. 4 Spatial distribution of seasonal root mean square error (rmse) rainfall (mm/day) based on day-1, day-3 and day-5 forecasts of GFS T382 (top panel) and GFS T574 (bottom panel) for the period from 1 June to 30 September 2011

4 Result and discussions

4.1 Rainfall prediction skill

4.1.1 Observed and forecast fields

We begin with a description of observed fields of rainfall for the season (1 June to 30 September 2011). Figure 2 (top panel) illustrates the spatial distribution of mean rainfall of the season based on the observations. The observed rainfall

distribution shows a north south oriented belt of heavy rainfall along the west coast with a peak of ~ 15 mm/day. The sharp gradient of rainfall between the west coast heavy rainfall and the rain shadow region to the east, which is normally expected, is noticed in the observed field. Another heavy rainfall belt (~ 20 mm/day) is observed over the North Bay of Bengal, extending from Myanmar coast to Orissa coast. A rainfall belt of order 10–15 mm/day is noticed over the eastern central parts of the country over the domain of monsoon trough. Rainfall of the order

to 10–15 mm/day is also observed over north-east India. Rainfall has been <5 mm/day over most parts of south peninsular India and extreme north-west India.

In general, the forecast fields (day-1, day-3 and day-5) of seasonal mean rainfall from GFS T382 (Fig. 2 middle panel) and GFS T574 (Fig. 2 bottom panel) could reproduce the heavy rainfall belts along the west coast, over the north Bay of Bengal extending up to Myanmar areas. However, some spatial variations in magnitude are noticed.

In the forecast by GFS T382, 15–20 mm/day rainfall is noticed along the west coast in the day-1, day-3 and day-5

forecasts, and an increasing trend with the forecast lead time. 15–20 mm/day rainfall belt lay over North Bay of Bengal, and the amount becomes 20–25 mm/day over Myanmar coast and adjoining areas. Over the north-east India and along the foot hills of the Himalaya, rainfall has been of the order of 15–20 mm/day. Rainfall has been of the order of 10–15 mm/day over the central India. Over the most parts of south peninsular India rainfall has been <5 mm/day.

In the forecast by GFS T574, 15–20 mm/day rainfall is noticed along the west coast in the day-1, day-3 and day-5 forecasts. A belt of 20–25 mm/day rainfall lay over north-

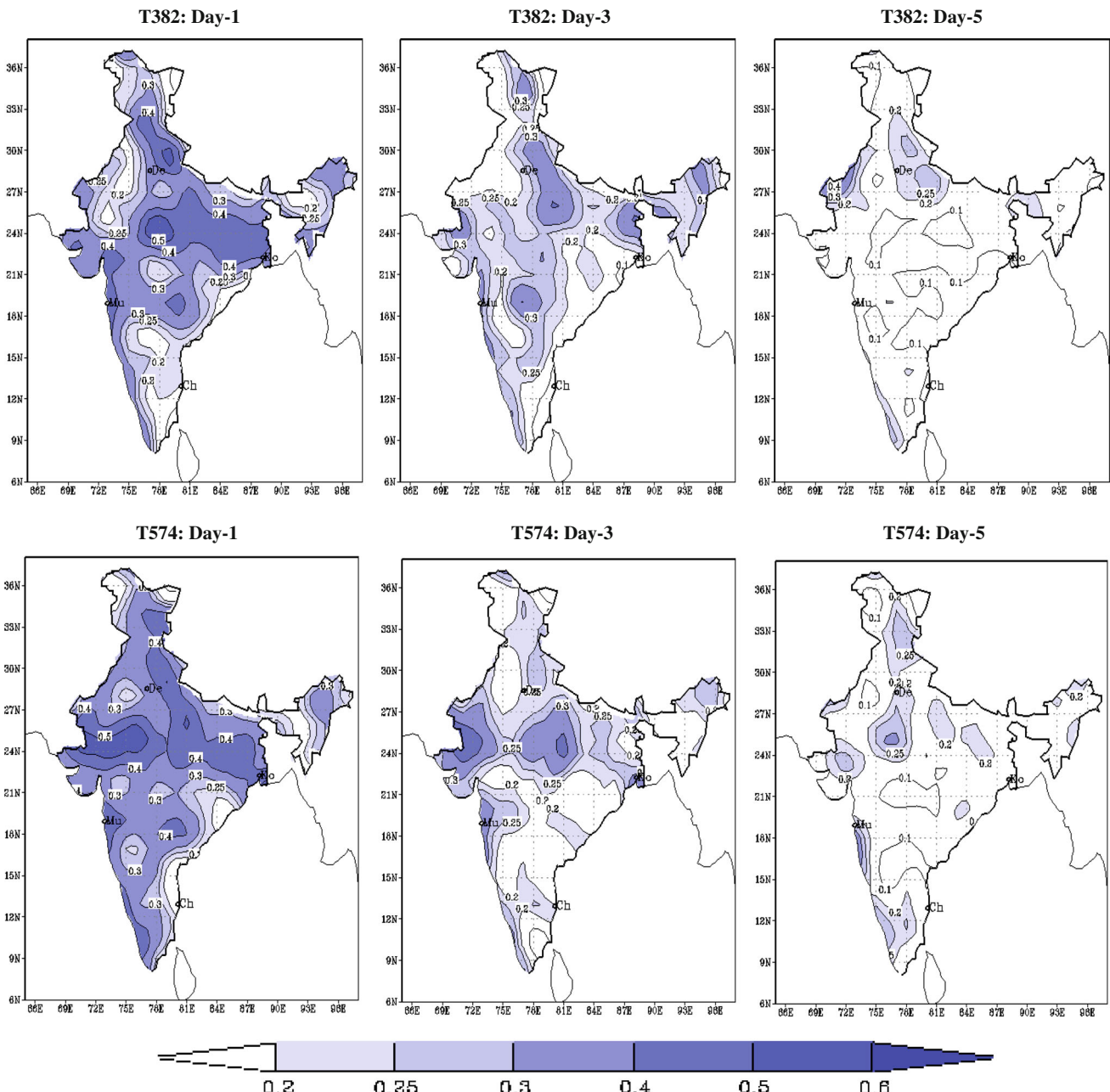


Fig. 5 Spatial distribution of anomaly correlation coefficient between the observed and the model predicted rainfall for day-1, day-3 and day-5 forecasts of GFS T382 (top panel) and T574 (bottom panel) for the period from 1 June to 30 September 2011

east India and over the Myanmar coast. Rainfall has been of the order of 10–15 mm/day over central India—neighboring regions and a decreasing trend with forecast lead time. Rainfall amount has been <5 mm/day over most parts of south peninsular India.

4.1.2 Spatial characteristics of forecast skills

In Fig. 3, the spatial distribution of seasonal mean errors (forecast-observed) of rainfall (mm/day) at the resolution of 50 km based on day-1, day-3 and day-5 forecasts of *GFS T382* (top panel) and *GFS T574* (bottom panel) for the period from 1 June to 30 September 2011 are demonstrated. Results of both *GFS T382* and *T574* show mean errors of the order of −5 to +5 mm/day for day-1, day 3 and day-5 forecasts over the country, except over the north-east India. Mean errors have been of the order of 15–20 mm/day over north-east India and over Myanmar coast and adjoining areas of north Bay of Bengal.

GFS T382 shows negative mean errors (<5 mm) over central India and North West Bay, over the domain of monsoon trough. Area of negative mean errors expands over most parts of the country with the forecast lead time. Large positive mean errors of the order of 10–15 mm/day lay over the central and adjoining south Bay of Bengal and also over south east Arabian Sea and an increasing trend with forecast lead time. *GFS T574* shows positive mean errors (<5 mm/day) over most parts of the country in the day-1 forecast, except over east central India and adjoining north-west Bay, over the domain of monsoon low. With the forecast lead time, area of negative mean errors spread over most parts of the country.

Seasonal mean error (Fig. 3) shows the systematic error of the model. However, while summing for the season, errors of opposite sign might be getting cancelled in some regions and the bias representation may not be fully informative. Hence, the mean error plots have to be examined in conjunction with the Root Mean Square Error (RMSE) plots for the said regions. The spatial distribution of seasonal RMSE of rainfall (mm/day) based on day-1, day-3 and day-5 forecast of *GFS T382*

(top panel) and *GFS T574* (bottom panel) for the period from 1 June to 30 September 2011 is shown in Fig. 4. The RMSE of day-1, day-3 and day-5 forecasts of the model has a magnitude between 1 and 20 mm, except over the Myanmar coast where the magnitude of RMSE exceeds 30 mm/day. Higher magnitude of RMSE (15–20 mm/day) are noticed over the domain of climatologically higher monsoon rainfall belts such as, west coast of India, north east India, central India—along the domain of monsoon trough and north-west bay of Bengal, over the domain of monsoon low. Magnitude of RMSE is found to be slightly higher for *GFS T574*, indicating higher random errors in the performance of the model.

The anomaly Correlation Coefficient (CC) between the observed and the model forecast rainfall for day-1, day-3 and day-5 of *GFS T382* (top panel) and *T574* (bottom panel) is shown in Fig. 5. The CC between trends in the forecast and observation is a measure of the phase relationship between them. Here, we have computed the anomaly CC by using daily data for the monsoon periods (June–September) of 122 days. The anomaly CC is statistically significant at the 99.9 % confidence level for a value of 0.3 and above. Over most parts of the country, the magnitude of day-1 forecast anomaly CC lies in between 0.3 and 0.5, while over the monsoon trough regions the magnitude of anomaly CC exceeds 0.5. This indicates that the trend in precipitation in the day-1 forecasts of the model is in good phase relationship with the observed trend over a large part of the country. A small area over south west Rajasthan has a magnitude of anomaly CC exceeding 0.6 in *GFS T574*. The magnitude of anomaly CC decreases with the forecast lead time, and by day 5 anomaly CC values over most parts of India are between 0.2 and 0.4, except in pockets near the east coast and south peninsular India where the anomaly CC values are below 0.1. For a sample size of 122 (monsoon days), the CC is statistically significant at the 99 % confidence level for values exceeding 0.239. Inter-comparison reveals that *GFS T574* has relatively higher anomaly CC than *T382* in all day-1, day-3 and day-5 forecast.

Fig. 6 Domain mean weekly (7 days accumulated) observed, climatology and (0–168 h) forecasted rainfall (mm) from *GFS T382* and *T574* over all India during monsoon 2011

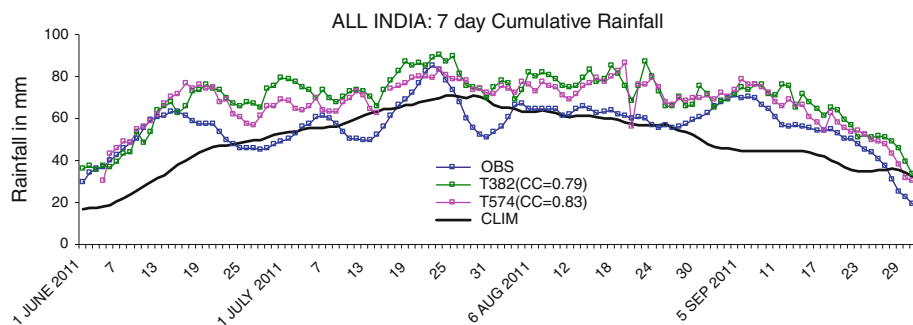
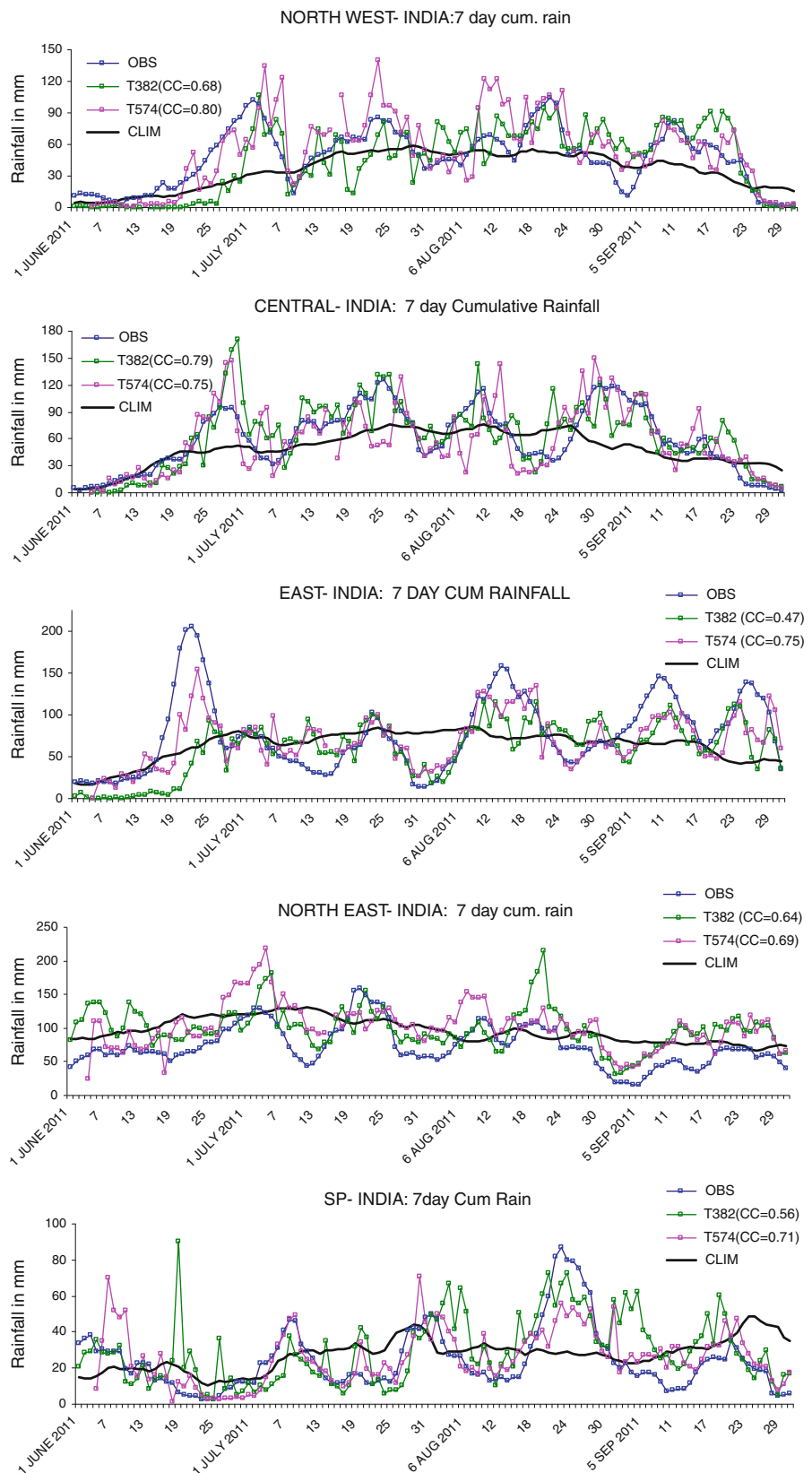


Fig. 7 Domain mean weekly (7 days accumulated) observed, climatology and (0–168 h) forecasted rainfall (mm) from GFS T382 and T574 over different homogeneous regions (NW, CE, EI, NE and SP) of India during monsoon 2011



4.1.3 Time series of weekly accumulated rainfall of daily forecasts

An inter-comparison of time series of daily country mean weekly (7 days) cumulative observed, climatology and corresponding (7 days) forecasted rainfall of GFS T382 and T574 over all India is presented in Fig. 6. Similar results for different homogeneous regions of India are presented in Fig. 7. The active and weak spell of rainfall activity is well reflected in the weekly rainfall of all India and also the weekly rainfall over different domains of India. The 7 days cumulative forecast of both GFS T574 and T382 are in phase (active/weak spell of rainfall) with the corresponding observed rainfall, indicating the predictability of rainfall in weekly time scale. The active rainfall activity (positive anomaly) and weak or break condition of rainfall activity (negative anomaly) is well captured by GFS T574 and T382 in weekly scale (Fig. 6). GFS T574 shows CC of 0.83 against the CC of 0.79 by GFS T382 over all India. Both GFS T574 and T382 show over-estimation of rainfall and magnitude of over-estimation is slightly higher in case of T382. For the north-west India GFS T574 shows CC of 0.80 against the CC of 0.60 by GFS T382, for central India GFS T574 shows CC of 0.77 against the CC of 0.76 by GFS T382, for east India GFS T574 shows CC of 0.75 against the CC of 0.47 by GFS T382, for north east India GFS T574 shows CC of 0.69 against the CC of 0.64 by GFS T382 and for south peninsular India GFS T574 shows CC of 0.71 against the CC of 0.56 by GFS T382. In case of northwest India, spells of ups and downs of rainfall activity are better captured by GFS T574. But it shows some over-estimation during July and August, where as T382 shows under-estimation. For central India, T574 shows some mismatch of rainfall spells during July and August. For east India, rainfall peaks are, in general, underestimated by both T574 and T382. For north-east India, both the models show over-estimation. For south peninsular India, GFS T382 shows many mismatch of rainfall spells.

In Fig. 8, an inter-comparison of CC between T574 and T382 for the 7 days cumulative rainfall against the observed rainfall for different homogeneous regions (central India, northwest India, north-east India, east India, southern peninsula, west coast of India and country as a whole) is presented. Inter-comparison clearly reveals that GFS T574 has better skill as compared to GFS T384 in all the homogeneous regions. In the regional spatial scale GFS T574 shows CC of order 0.7 and above.

An inter-comparison of CC for day-1 to day-5 forecasts by IMD GFS T382 and T574 for the country is shown in Fig. 9. The values of CC decrease ranging from 0.85 at day-1 to 0.70 at day-5 forecast. The results show that the GFS T574 has higher skill than that of T382 at all forecast days, particularly at day-2, day-3 and day-4 forecasts.

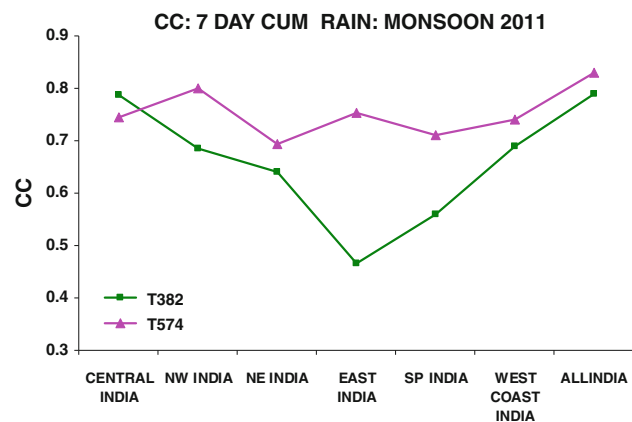


Fig. 8 Domain mean correlation coefficient (CC) of weekly (7 days) cumulative observed and corresponding 7 days cumulative forecasts of rainfall by GFS T382 and T574 for different homogeneous regions of India during monsoon 2011

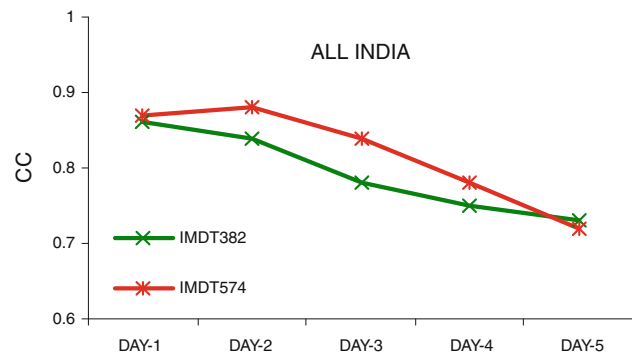
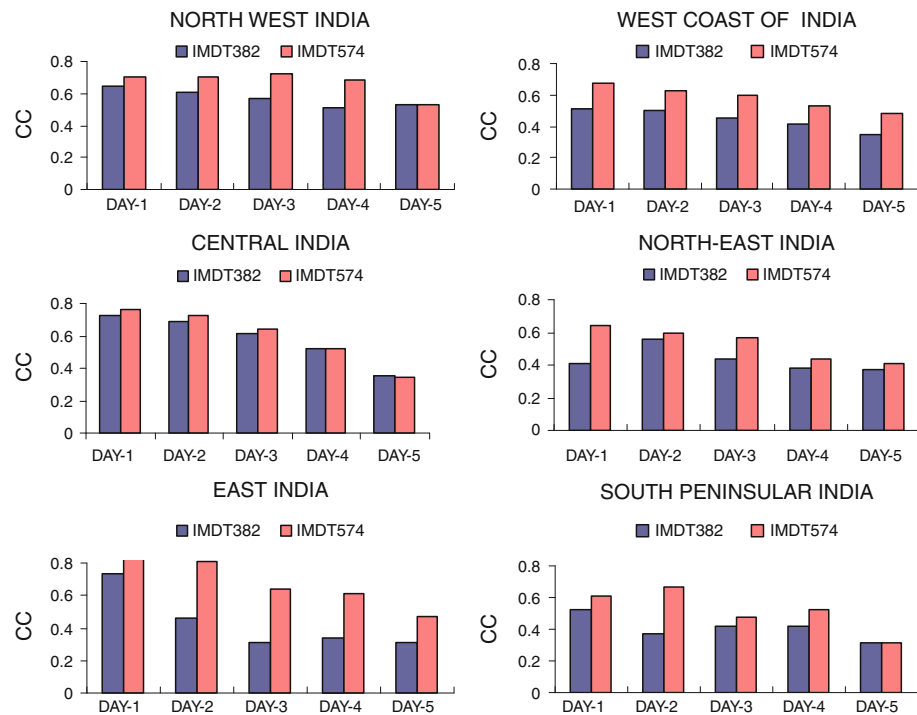


Fig. 9 Correlation coefficient of all India daily mean observed and corresponding forecast rainfall of day-1 to day-5 by GFS T382 and GFS T574 during monsoon 2011

The CC for day-1 to day-5 forecasts of different homogeneous regions of India are shown in Fig. 10. For the north-west India CC for T382 ranges from 0.60 at day-1 forecast to 0.55 at day-5 forecast. The CC has been 0.10 higher in the T574 for the forecast up to day-4 and becomes equal at day-5 forecast. For the West coast of India CC for T382 ranges from 0.50 at day-1 forecast to 0.40 at day-5 forecast. The CC has been 0.20–0.30 higher in the T574 at all forecasts of day-1 to day-5. In central India, both for T382 and T574, the CC ranges from 0.75 at day-1 to 0.4 at day-5. The CC for T574 was slightly higher at day-1 and day-2 forecasts. For the north east India CC remains around 0.40 at all forecast days for T382. In the T574 the CC has been 0.1–0.30 higher at all forecasts. For south peninsular India, CC remains around 0.40 for T382. It has been 0.3–0.1 higher in the T574 forecasts.

The results show that the GFS T574 has relatively higher skill (at the regional spatial scale) than T382 at all forecast days. This indicates that the trend in domain mean daily rainfall in the day-1 to day-5 forecasts of the GFS

Fig. 10 Correlation coefficient of daily mean observed and corresponding forecast rainfall by GFS T382 and T574 (for day-1, day-2, day-3, day-4 and day-5) over different homogeneous regions of India during monsoon 2011



T574 model has been in the better phase relationship with the observed trend over most parts of the country.

4.1.4 Categorical statistical skill scores

The rainfall forecast skills are highly depend on the resolutions of verified grids/boxes (spatial) and time period (temporal). A spatially (domain) averaged field always has lower variability than grid point values. The standard deviation of an observed/forecast field reduces when the field is spatially averaged at higher spatial scales. As the scale of spatial averaging becomes larger, the true areal averages themselves will become less variable and will be more accurately estimated by the averages coming from the grid point values. So, any NWP model has higher skill (lower variability) at larger spatial scale or weekly time scale as compare to smaller spatial scale or daily time scale. There is higher skill if the verified grids/boxes are very large or the time period is very long. The average of the forecast errors over a long period of time is a measure of the systematic part of the forecast error, while root-mean-square error (RMSE) is a measure of the random component of the forecast error. The correlation coefficient between trends in the forecast and observation is a measure of the phase relationship between them. The statistical parameters based on the frequency of occurrences in various classes are more suitable for determining the skill of a model in

predicting precipitation. The aspect of model behaviour is further explored in Fig. 11 with probability of detection (POD), which is also called hit rate, and in Fig. 12 with bias score for classes with class marks of 0.1, 1, 2, 5, 10, 15, 35,..., 65 mm. These skill scores are computed at the grid resolution of 50 km over the country.

The probability of detection (POD) is equal to the number of hits divided by the total number of rain observations; thus it gives a simple measure of the proportion of rain events successfully forecast by the model. From Fig. 11, it is seen that the probability of detection is more than 50 % for class marks below 10 mm/day for day-3 and day-5 forecast of both GFS T382 and T574, but the POD score of GFS T574 is little higher than GFS T382 in all the threshold ranges over the country. It is also seen that skill is a strong function of threshold as well as forecast lead time, with the probability of detection (POD) decreasing from about 80–90 % for rain/no rain (>0.1 mm/day) to about 20 or 30 % for rain amounts above 30 mm/day.

The bias of a model forecast is the ratio of the predicted number of occurrences of an event to the number of occurrences of the same event actually realized in nature. It measures the ratio of the frequency of forecast events to the frequency of observed events. Indicates whether the forecast system has a tendency to under forecast ($\text{BIAS} < 1$) or over forecast ($\text{BIAS} > 1$) events. It does not measure how well the forecast corresponds to the observations, only

Fig. 11 Hit Rate for day-3 and day-5 forecast of GFS T382 and T574 over India during monsoon 2011

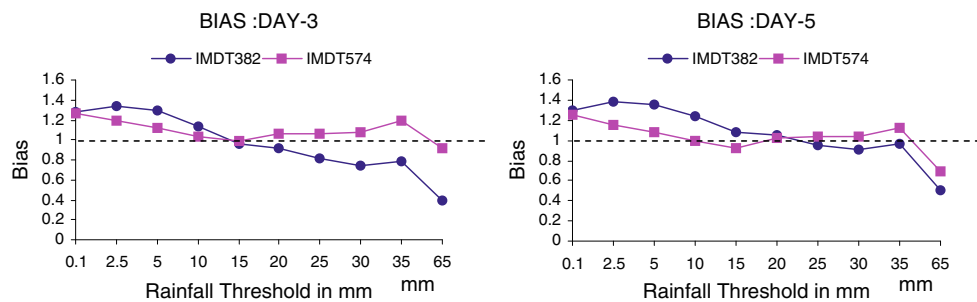
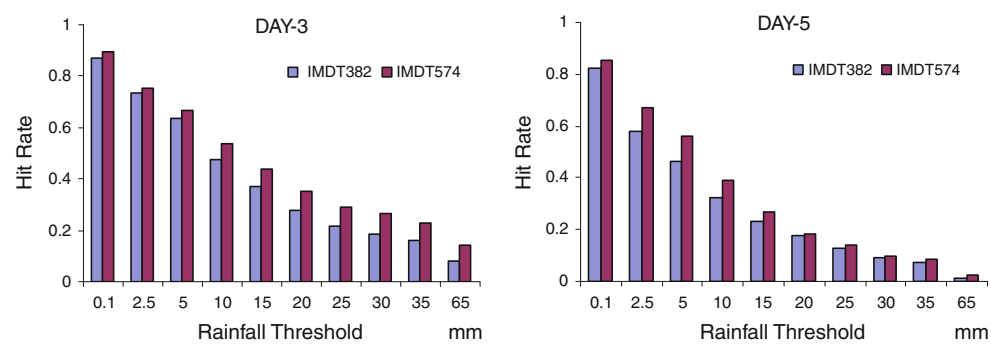


Fig. 12 Bias score for day-3 and day-5 forecast of GFS T382 and T574 over all India domain during monsoon 2011

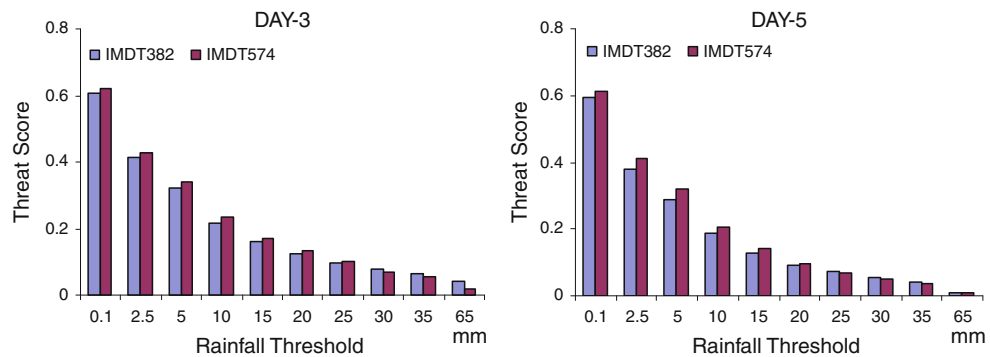
measures relative frequencies. Figure 12 shows the day-3 and day-5 bias of the GFS T382 and T574 model. Both the day-3 and day-5 bias of GFS T382 over predicts (bias > 1) in the low threshold ranges up to 20 mm and under predicts (bias < 1) rainfall event in the higher threshold ranges. While, the GFS T574 day-3 and day-5 bias over predicts (bias < 1) rainfall event only up to 20 mm and above 20 mm the bias score is closer to 1.0.

Threat score (TS), also known as the critical success index (CSI, e.g., Schaefer 1990); is the ratio of the number of correct model prediction of an event to the number of all such events in both observed and predicted data. It can be thought of as the accuracy when correct negatives have been removed from consideration, that is, TS is only concerned with forecasts that count. Sensitive to hits, penalizes both misses and false alarms. It does not distinguish the source of forecast error and just depends on the climatology frequency of events (poorer scores for rarer events) since some hits can occur purely due to random chance. The higher value of a threat score indicates better prediction, with a theoretical limit of 1.0 for a perfect model. The threat score (TS) for day-3 and day-5 forecast of GFS T382 and GFS T574 for monsoon 2011 is shown Fig. 13. The threat score starts close to 0.65 and then decreases to 0.3 near the 15 mm mark. The day-3 and day-5 TS of GFS T574 is slightly higher than GFS T382 in the lower and medium threshold ranges up to 25 mm/day. GFS T574 has slightly lower TS skill than GFS T382 in the higher

threshold ranges of 30 and 35 mm/day. The number of data point (n) over Indian land area is 4485 (x axis 69 and y axis 65) and the standard deviation of TS for T574 and T382 is in the range from 0.13 to 0.16 for different threshold ranges. The statistical significance test for TS (Fig. 13) is carried out using student's t test over all India and found that this difference in TS between T574 and T382 at all threshold range is extremely statistically significant at 95 % confidence level.

ETS is used for the verification of rainfall in NWP models because its equitability allows scores to be compared more fairly across different regimes. If ETS = 1, it indicates that there is no error in the forecasting. ETS = 0 indicates that none of the grid points are correctly predicted. Figure 14 shows ETS skill score of GFS T382 and GFS T574 for rainfall threshold of (a) 5 mm/day and (b) 15 mm/day for the homogeneous regions of India. ETS skill for rainfall threshold of 5 mm/day for GFS T574 is slightly higher than GFS T382 model in all the regions of study. ETS skill score is relatively high (order of 0.2–0.25) over west coast of India, where the rainfall variability is high. ETS skill is low over NE India for both the rainfall threshold of 5 mm/day and 15 mm/day. GFS T574 has slightly higher ETS skill than GFS T382 in all the regions. Interestingly, the day-1 to day-5 ETS score of GFS T574 remains relatively higher than GFS T382 in all thresholds and domains of study. The statistical significance test for Equitable Threat Score (ETS) in Fig. 14 is also carried out

Fig. 13 Threat score for day-3 and day-5 forecast of GFS T382 and T574 over all India domain during monsoon 2011



over all India and five homogeneous regions of India. The number of data point over Indian land area is 4485 and the standard deviation in ETS is in the range from 0.05 to 0.09 for different threshold ranges, whereas the number of data point over five homogeneous regions are 121 (x-axis 11 and y-axis 11) and the standard deviation in ETS is in the range from 0.02 to 0.06 for different threshold ranges. The difference in ETS between T574 and T382 is statistically significant at 95 % confidence level for all the regions and at all the threshold ranges except over west coast of India at 5 mm/day threshold range in day-2 and day-3 forecast.

The error characteristics reflected in the results of categorical statistics is a common problem with any numerical models (Schultz 1995; Wang and Seaman 1997; Belair et al. 2000). At the high precipitation categories, the coarse-grid forecasts substantially under predict the rain amounts. This can be attributed to the coarse-grid global model resolution (0.23°), which does not permit the correct representation of fine-scale convective motions that usually give the highest precipitation amounts.

4.2 Monsoon circulation features

In order to understand the characteristic features of monsoon captured by the model, in first part of this section, the model performance is examined in terms of vertical structure of specific humidity, spatial distribution of precipitable water content and lower tropospheric circulation. To assess the ability of the model to capture features of monsoon depression, an episode of a monsoon depression and associated heavy rainfall is also illustrated in the second part of this section.

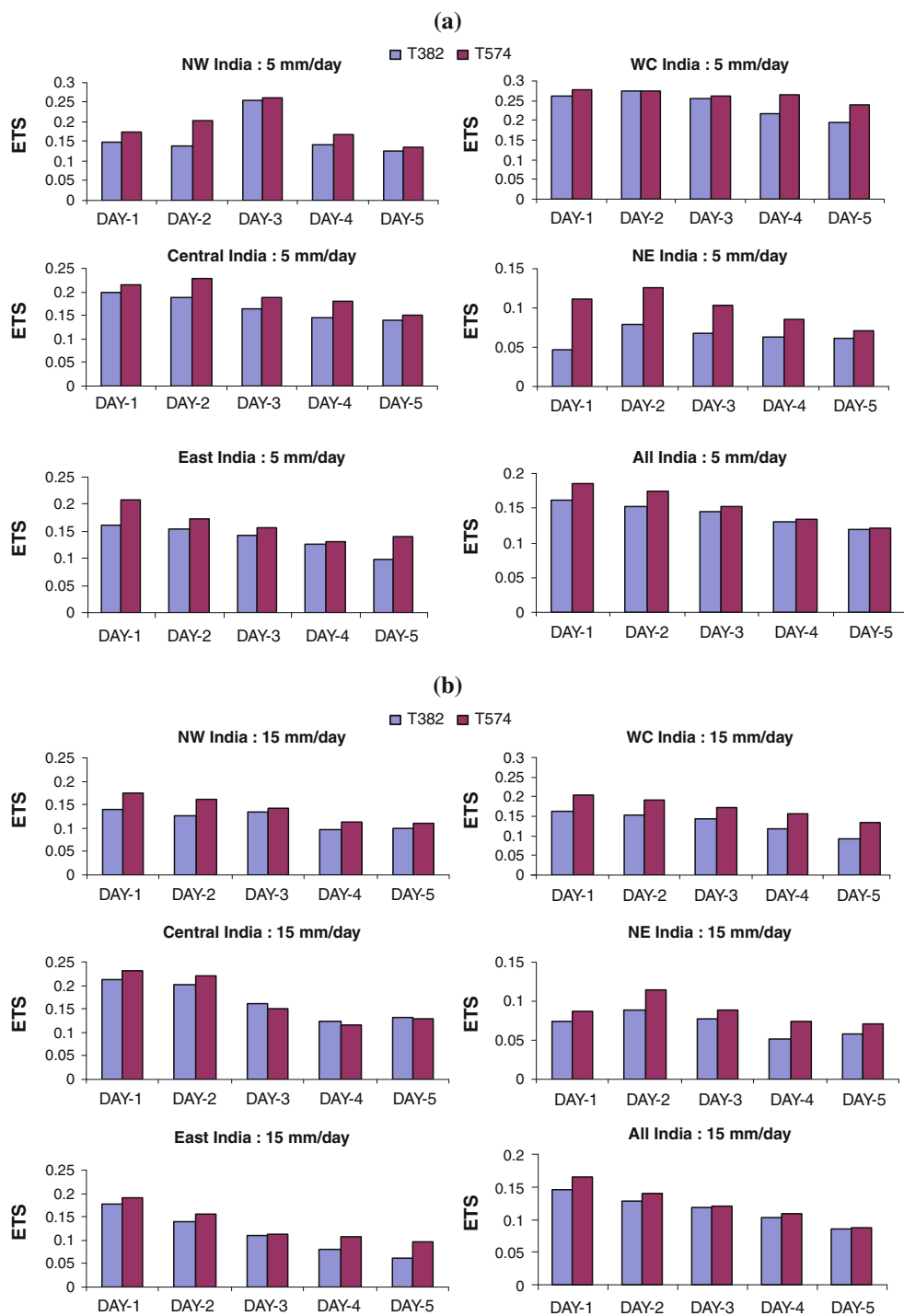
4.2.1 Seasonal moisture fluxes

In Fig. 15, zonally averaged (long 60°E – 100°E) specific humidity (g/kg) of analysis, day-1 and day-3 forecast errors from GFS T574 and GFS T382 for monsoon 2011 are presented. Both the analysis shows similar pattern with

highest value of specific humidity (16 g/kg) below 950 hPa, which becomes 4 g/kg at around 600 hPa. There is a vertical extension of higher value of specific humidity between lat 25°N and 30°N . GFS T574 forecast errors shows negative bias between 850 and 650 hPa, extending northward up to 30°N with two minima, one at the equator and another between 15°N and -20°N around 800 hPa. In the lower levels from surface between lat 10°N and 15°N , there is a negative bias of specific humidity. Above 550 hPa, the error is positive with a maximum value between 600 and 500 hPa and lat 10°N – 15°N . The magnitude of bias increases with the forecast lead time. GFS T382 shows negative bias below 850 hPa with a minimum value at 950 hPa between lat 5°N – 10°N hPa and a strong positive bias above 850 hPa with a large domain of maximum value at 700 hPa between lat 5°N – 10°N . A significant difference is noticed in the mean errors of these two forecasts.

Figure 16 presents seasonal mean precipitable water content (PWC; in mm) analysis and mean error of day-1, day-3 and day-5 forecasts from GFS T574 and GFS T382. PWC of higher magnitudes (60–65 mm) is located over the North Bay of Bengal and adjoining areas of east India and neighboring states. PWC of order 55–60 mm is found along foot hills, along the monsoon trough region, west coast of India and central Bay of Bengal. Similar pattern is noticed in the corresponding T382 analysis. In the T574, day-1 forecast error (Fig. 16) shows negative error of order -2 to -3 mm along the region of south of the monsoon trough, some pockets over north west India, north-east India. A pocket of positive error is noticed over western part of the country and along the foot hills of Himalaya. The pattern remains same in the day-3 and day-5 forecasts, but with increasing magnitude of negative errors. The pattern of PWC mean error is found to be broadly matching with the corresponding mean error (under-estimation) pattern of rainfall over India. A significant difference is noticed in the error pattern of PWC forecasts between GFS T574 and GFS T382. In the GFS T382, a belt of positive

Fig. 14 Equitable threat score (ETS) of GFS T382 and T574 for rainfall threshold of **a** 5 mm/day and **b** 15 mm/day for the homogeneous regions of India



error is noticed over north east Arabian Sea and adjoins western parts of the country. A pocket of positive error is also noticed along the foot hills of Himalaya. A belt of negative errors are found across the country along 20°N, over north east India and along northern parts of east coast. The pattern remains same in the day-3 and day-5 forecasts with increasing magnitude of positive errors. The negative

mean error of PWC over the central part and over east coast is in well agreement with the responding pattern of mean error of rainfall. But it is difficult to explain the reason for large positive mean error of PWC over the north east Arabian sea extending northward over the land.

In Fig. 17, Seasonal (JJAS) mean wind direction (arrows) and wind speed (color shading) (in m/s) at 850 hPa analysis

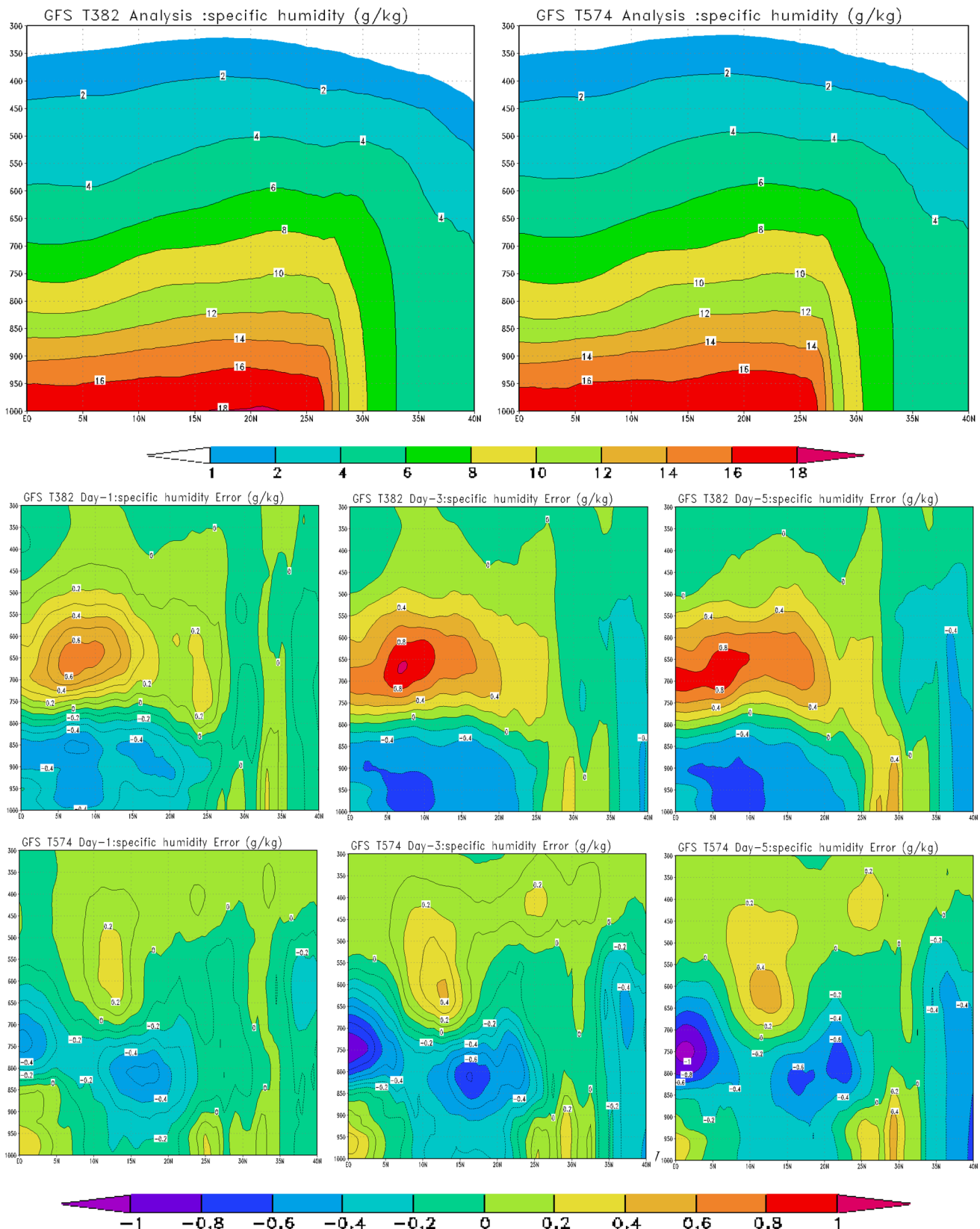


Fig. 15 Zonally averaged (long: 60–100E) specific humidity (g/kg) analysis (*top panel*); 24 72 and 120 h forecast error in specific humidity (g/kg) from GFS T382 (*middle panel*) and GFS T574 (*bottom panel*) for monsoon 2011

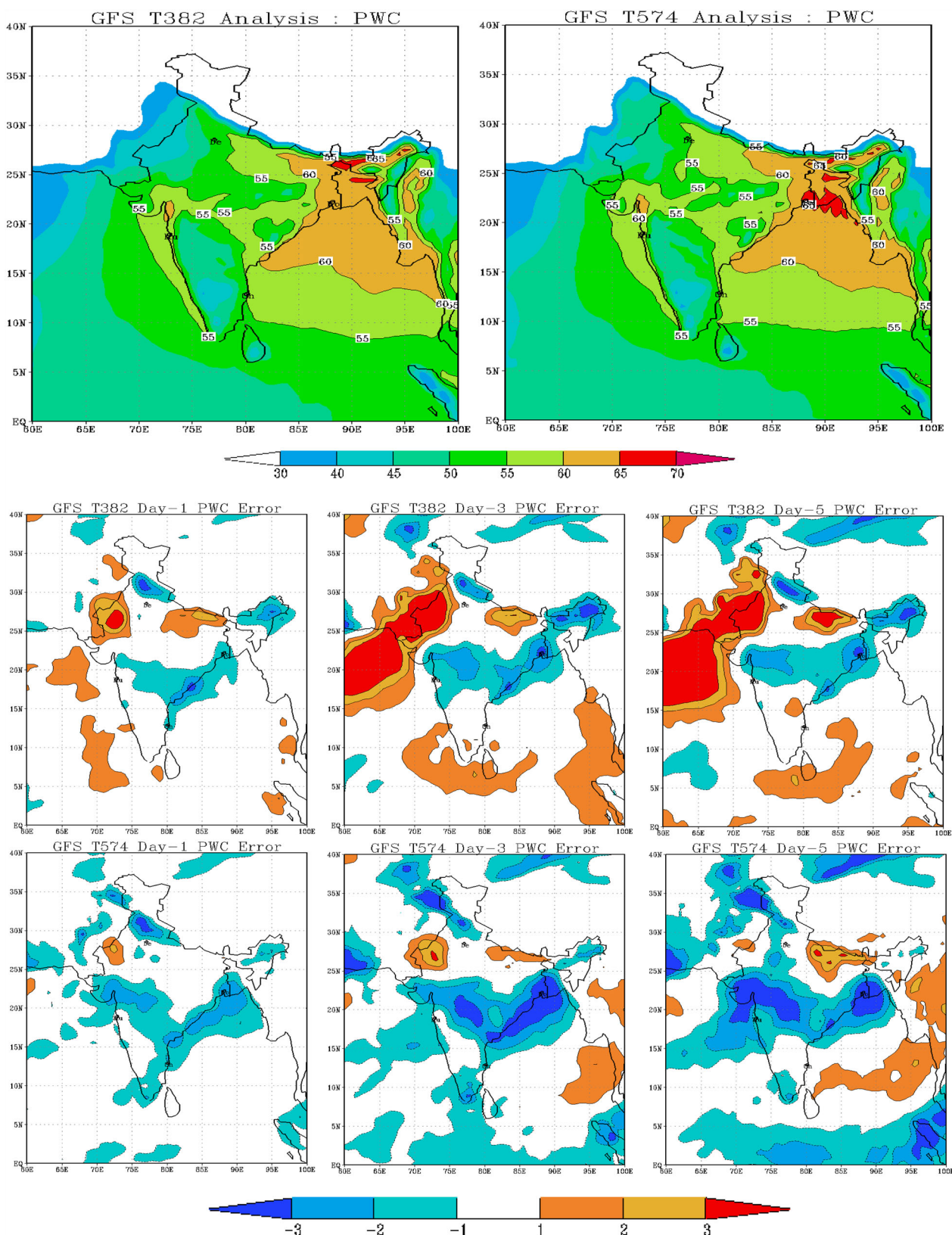


Fig. 16 Seasonal (JJAS) mean precipitable water content (PWC in mm) analysis (*top panel*) and mean error of PWC 24, 72 and 120 h forecast from GFS T382 (*middle panel*) and GFS T574 (*bottom panel*) for monsoon 2011

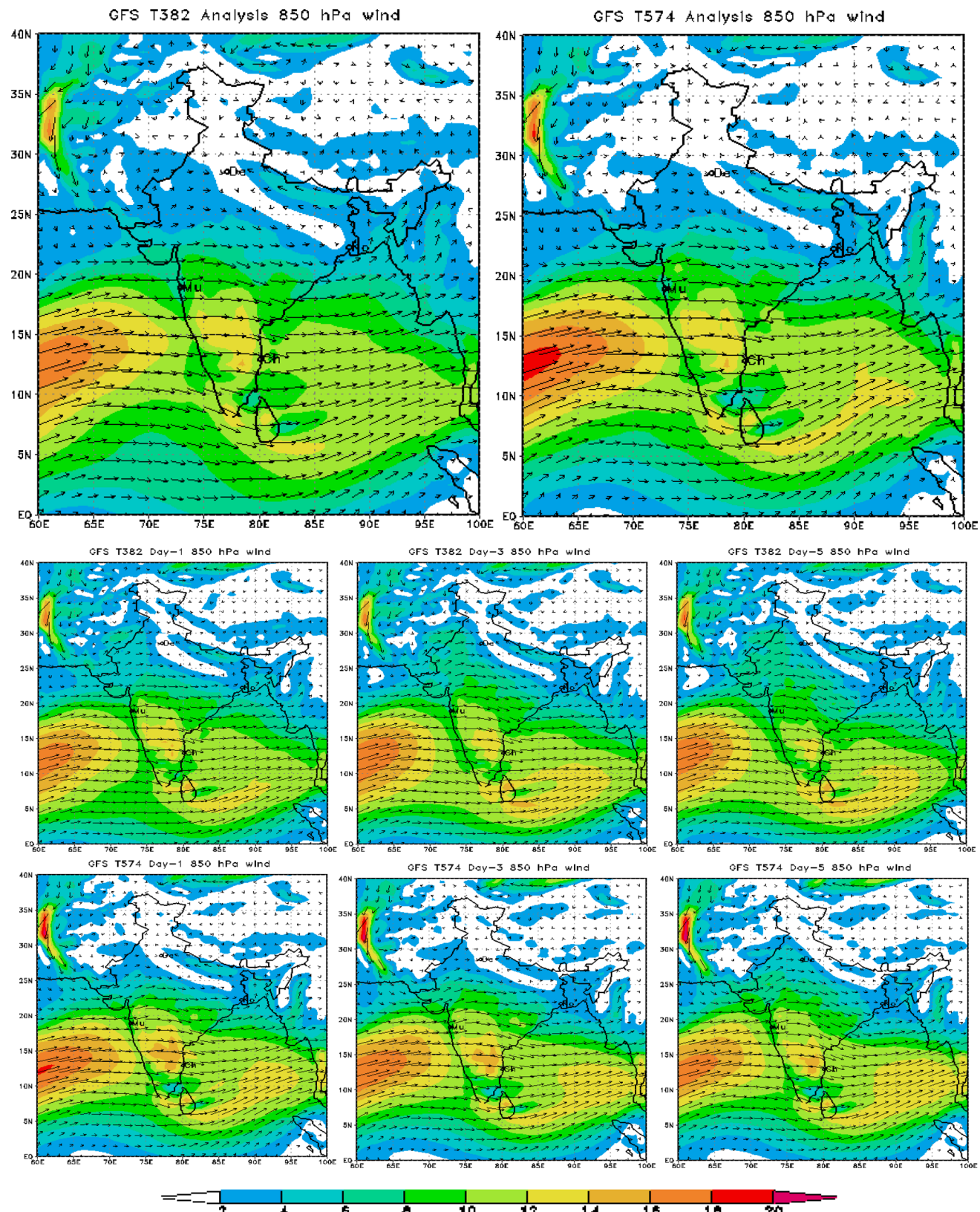


Fig. 17 Seasonal (JJAS) mean wind direction (arrows) and wind speed (color shading) (in m/s) at 850 hPa analysis (*top*) and 24, 72 and 120 h forecast of the GFS T382 (*middle panel*) and GFS T574 (*bottom panel*) for monsoon 2011

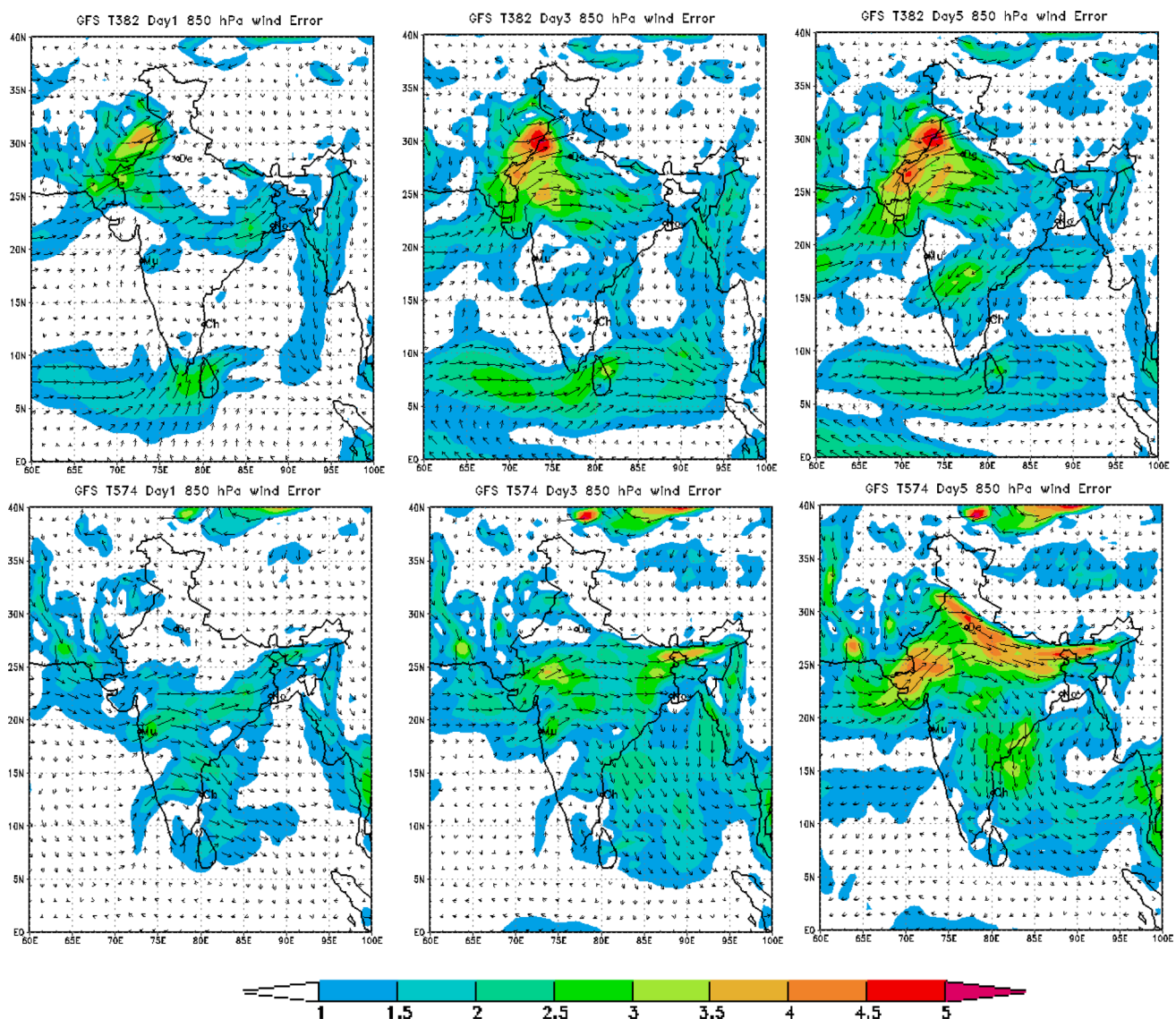


Fig. 18 Seasonal (JJAS) mean bias (forecast-analysis) in wind direction (arrows) and wind speed (color shading) (in m/s) at 850 hPa of 24, 72 and 120 h forecasts from GFS T382 (top panel) and GFS T574 (bottom panel) for monsoon 2011

(top) and 24, 72 and 120 h forecast of the GFS T382 (middle panel) and GFS T574 (bottom panel) for monsoon 2011 are presented. The 850 hPa wind analysis of both GFS T382 and T574 could capture low level westerly jet with a peak strength over the south west Arabian sea and the monsoon trough extending from northwest Bay of Bengal to northwest wards across the country. The low level jet is found to be slightly stronger in the GFS T574 analysis compared to GFS T382 analysis. Seasonal (JJAS) mean bias (forecast-analysis) in wind direction (arrows) and wind speed (color shading) (in m/s) at 850 hPa of 24, 72 and 120 h forecast from GFS T382 (top panel) and GFS T574 (bottom panel) for monsoon 2011 is shown in Fig. 18. Both GFS T574 and T382 show a bias anti-cyclonic circulation over the central India. GFS T574 forecast shows bias of westerly wind over most

parts of the parts of country extending up to the foot hills (indicating weak monsoon trough) south-westerly bias over the north west India and northeast Arabian sea, and northerly bias over east coast of India and adjoining Bay of Bengal extending southwards up to 15°N. Over the Myanmar it has been westerly bias. The magnitude of bias is found to grow with the forecast lead time. GFS T382 shows strong south-westerly bias over northwest India and adjoining Pakistan. In this case also considerable difference is noticed between the forecast errors of GFS T574 and GFS T382.

4.2.2 A case study of monsoon depression

In order to assess the ability of the model to capture features of monsoon depression, an episode of a monsoon depression

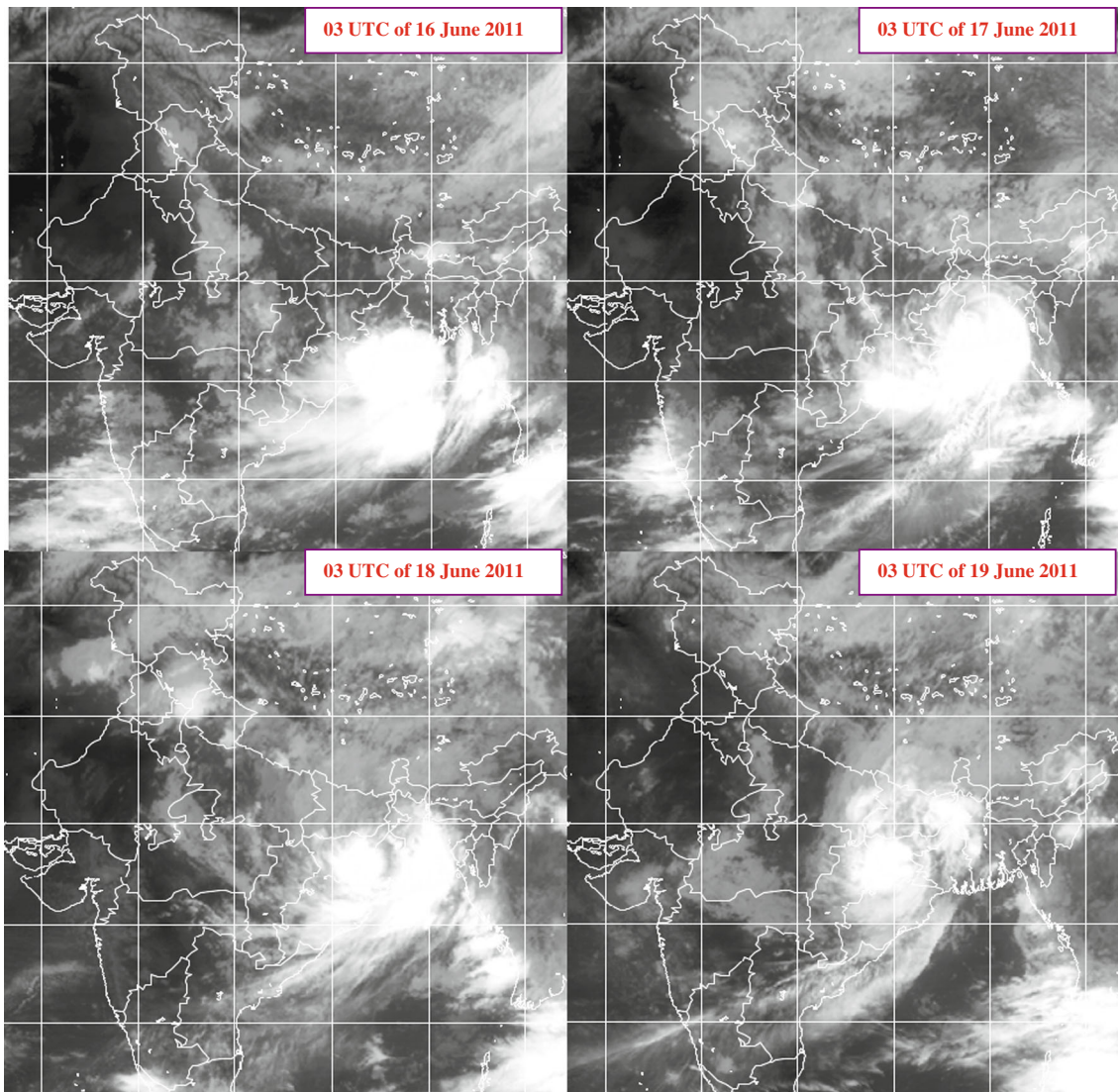


Fig. 19 Typical Satellite imageries at 0300 UTC of 16–19 June 2011

is illustrated. During summer monsoon 2011, there are four depressions formed. Out of these, two depressions that formed on 11th June over Arabian Sea and the other during 22nd–23rd, July over Land had a short life span. The monsoon depression formed during 16th–23rd, June and its subsequent west northwestward movement was responsible for the advance of the monsoon over the most parts of the country. The fourth monsoon depression formed towards the end of the season (22nd–23rd, Sept) weakened before moving towards northeast and no cyclone formed during the period. So, we have studied the main depression formed during 16–23, June in this paper. The satellite imageries of 16–19 June 2011 (Fig. 19) shows presence of a deep depression over the north Bay of Bengal on 16 June 2011, which crossed west Bengal-Bangladesh coast in the afternoon of 16 June 2011. It then continued northward movement for some time, and then moved west-northwestwards

across the country up to the central parts of India during 17–23 June and weakened gradually into a well marked low pressure area on 23 June. An inter-comparison of forecast track positions and the observed track is shown in Fig. 20. In the GFS T382 analysis, initial track position error (Fig. 21a) is about 150 km, which is only 50 km in the GFS T574. The position error has been within 150 km for forecasts up to 48 h in the GFS T574. Due to large initial error, GFS T382 continued to show larger track errors at 12 and 24 h also. At 36, 48 and 60 h both the models showed same track errors. At 72 h forecast GFS T574 showed 230 km errors where as GFS T382 showed 300 km position errors. The quantitative inter-comparison of track (Fig. 21a) and intensity (Fig. 21b) reveals that there is a considerable improvement in the track forecasts of day-1 to day-3 by GFS T574. This may be due to the vortex relocation algorithm, which is available in the GDAS of T574.

Fig. 20 Observed and model predicted tracks for deep depression (16–22 June 2011) from GFS T382 and GFS T574

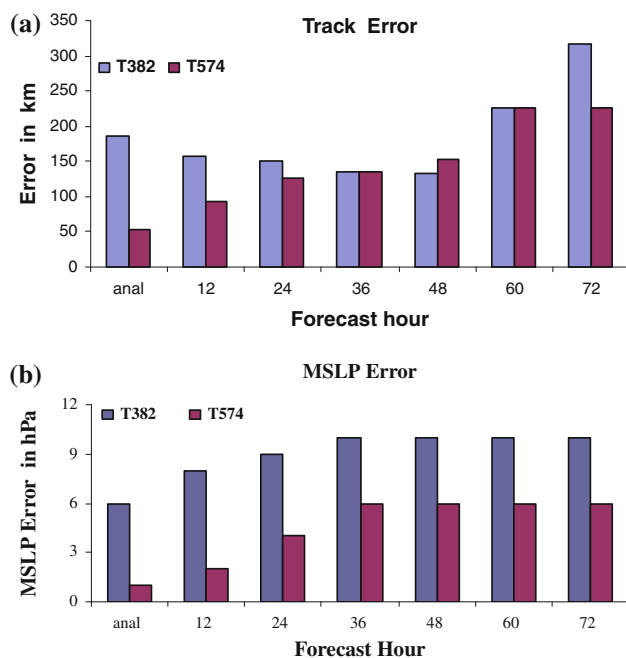
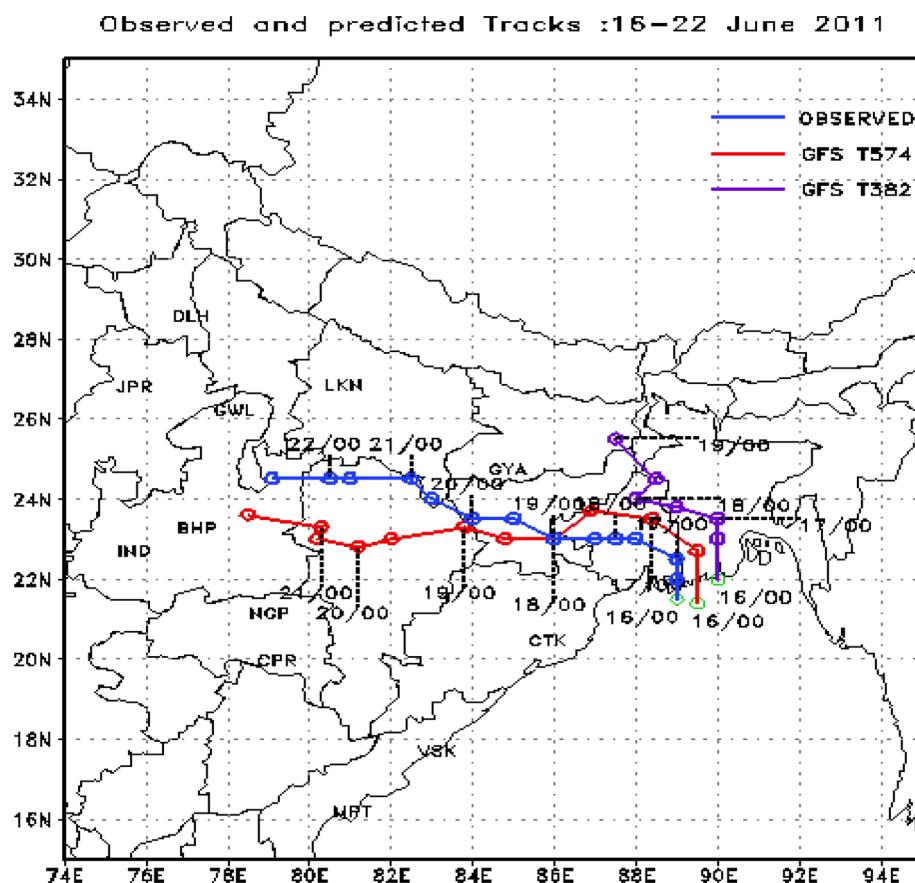


Fig. 21 **a** Track errors, **b** intensity (MSLP) errors of GFS T382 and GFS T574 for deep depression over Bay of Bengal (BOB) during 16–22 June 2011

The spatial distributions of MSLP along with specific humidity and wind at 850 hPa in relation to movement of the system and occurrences of heavy rainfall during 17–19 June are examined. It ushered southwest monsoon over eastern and central India and caused excess rainfall over these regions. The depression was responsible for the advance of the monsoon over the most parts of the country. The formation and intensity of this system have been better captured by the GFS T574 wind and specific humidity (in g/kg) at 850 hPa and MSLP based on 16th June 2011 initial condition as compared to GFS T382, as illustrated in Fig. 22. The movement of this low pressure system has been better forecasted up to day-3 (valid for 17, 18 and 19 June 2011) by GFS T574 as compared to GFS T382, as demonstrated in Fig. 22. GFS T574 model showed considerable skill in predicting the tropical cyclogenesis over the Bay of Bengal. However, the accuracy in prediction of location and intensity fluctuates considerably.

Under the influence of this monsoon depression, wide spread heavy rainfall activities occurred over central India during 20–23 June 2011. On 23 June 2011, number of places reported heavy to very heavy rainfall. Figure 23 shows the spatial distribution of gridded observed rainfall and 850 hPa wind analysis (top panel) along with day-1,

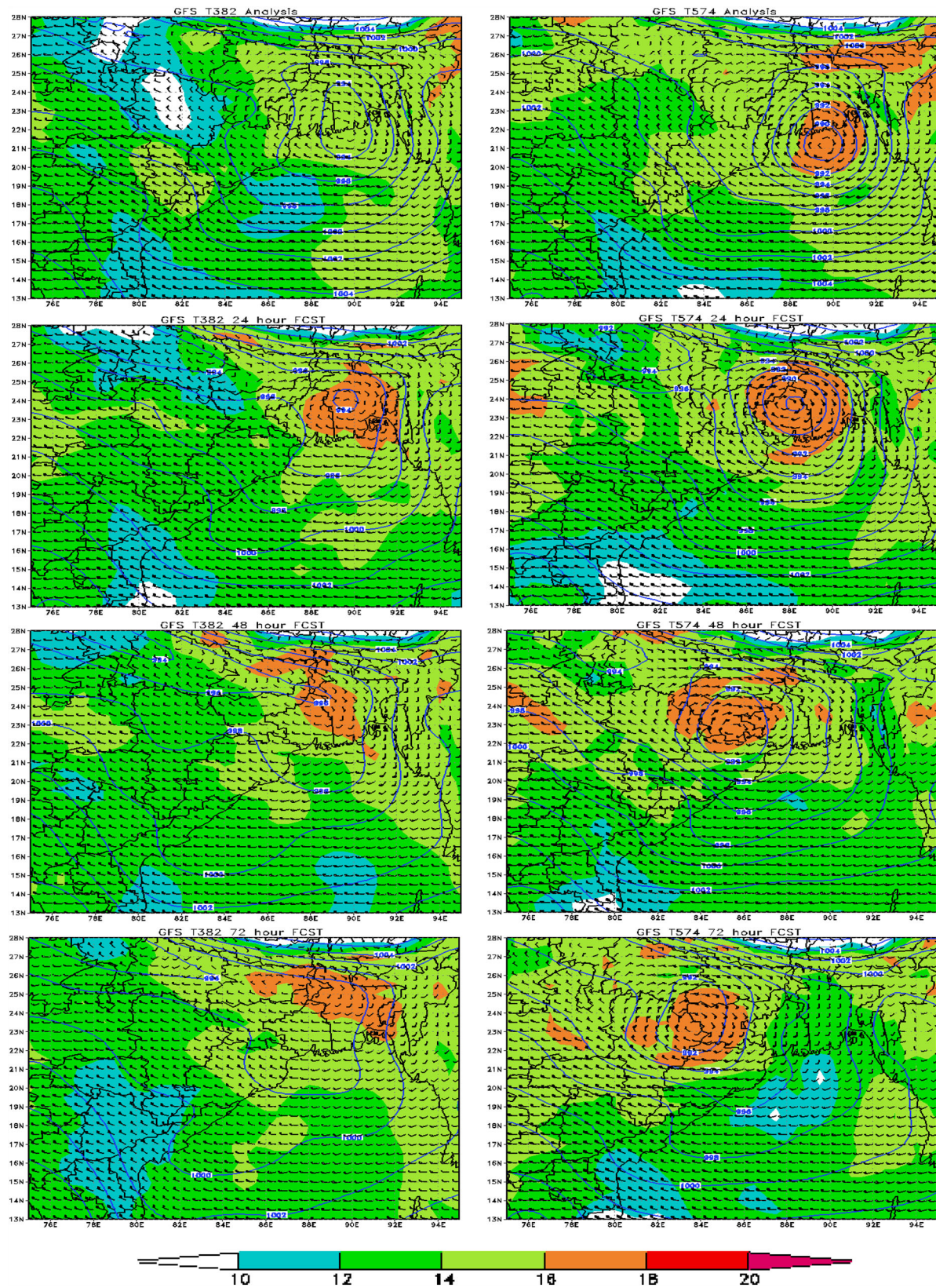


Fig. 22 850 hPa wind along with MSLP (in hPa) and specific humidity (in g/kg) analysis (16 June 2011); 24, 48 and 72 h forecast from GFS T382 (left panel) and GFS T574 (right panel) for 17, 18 and 19 June 2011 respectively

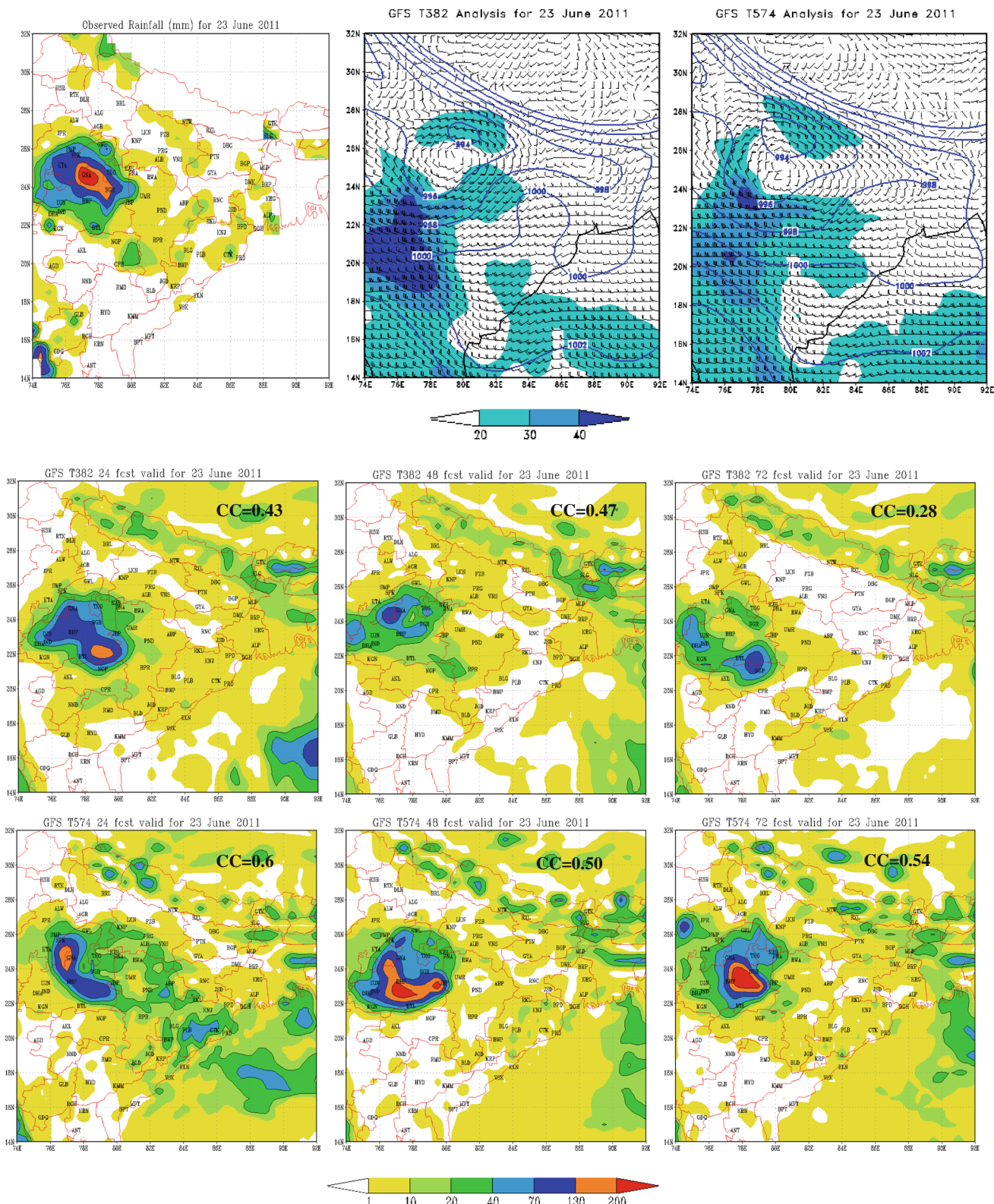


Fig. 23 Observed rainfall and 850 hPa wind analysis (top panel); 24, 48 and 72 h rainfall forecast from GFS T382 (middle panel) and GFS T574 (bottom panel) for heavy rainfall on 23rd, June 2011 over central India

day-2 and day-3 forecast rainfall from GFS T382 (middle panel) and GFS T574 (bottom panel) valid for 23 June 2011. The spatial CC for the country computed at the resolution of 50 km, shows that the CC for GFS T574 has been considerably higher compared to that of GFS T382 at all the forecasts (day-1, day-2 and day-3) valid for 23 June 2011. The spatial CC has been 0.60, 0.50 and 0.54 for the day-1, day-2 and day-3 forecasts by GFS T574. For GFS T382, it has been 0.43, 0.47 and 0.28 respectively at day-1, day-2 and day-3 forecasts. This clearly shows that the spatial distribution of rainfall of 23 June in association with this depression over central India is better captured by GFS T574. This suggests that the GFS T574 model forecast provides useful guidance for real time forecasting of heavy rainfall in association with monsoon depression.

5 Summary and concluding remarks

NCEP based Global Forecast System has been in operational use at IMD New Delhi for daily medium range forecasts. This paper assesses the performance of GFS T574 and GFS T382 to provide rainfall forecasts over Indian region in spatial and temporal scale during summer monsoon season of 2011. Performance of the model is examined in terms of vertically integrated moisture flux, lower tropospheric wind circulation and precipitable water content to understand the monsoon rainfall features captured by the model. The performance of the model during the episode of a monsoon depression is also illustrated in this study. The verification statistics for GFS T382 and T574 forecasts of upper air variables like wind, temperature and geo-potential height are also discussed for different regions of the globe.

The verification of rainfall is done in the spatial scale of 50 km, in a regional spatial scale and also country as a whole in terms of skill scores, such as mean error, root mean square error, correlation efficient, time series and categorical statistics such as, POD, bias score and ETS. The study demonstrates that the performance of GFS T574 and GFS T382 in predicting rainfall varies with geographical location and synoptic regime. For both the model, mean errors have been of the order of 15–20 mm/day over north-east India and over Myanmar coast and adjoining areas of North Bay of Bengal. With the forecast lead time (from day-2 onward), area of negative mean errors spread over most parts of the country. Magnitude of RMSE is found to be slightly higher for GFS T574, indicating higher variability in the performance of the model. Validation results shows that both the GFS T382 and T574 model forecasts, in general, are skillful over the regions of climatologically heavy rainfall domains. However, the accuracy in prediction of location and magnitude of rainfall

fluctuates considerably. Both the model forecasts have reasonably good capability to capture large scale rainfall features of summer monsoon, such as heavy rainfall belt along the west coast, over the domain of monsoon trough and along the foot hills of the Himalayas. In general, both the model showed considerable skill in predicting the daily and weekly accumulated rainfall amounts when averaged over the country. However the quantitative inter-comparisons of these results have clearly demonstrated the superiority of GFS T574 against the GFS T382.

No appreciable difference is noticed between the analysis fields of GFS T574 and GFS T382 in terms of vertically integrated moisture flux, PWC, zonally averaged specific humidity and lower tropospheric wind pattern. But in the corresponding forecast errors considerable differences between GFS T574 and T382 are noticed. Both version of model shows lower tropospheric drying and upper tropospheric moistening bias over Indian monsoon region. A bias of anti-cyclonic circulation in the lower tropospheric level lay over the central India, where rainfall as well as precipitable water content shows negative bias. Considerable differences between GFS T574 and T382 are noticed in the structure of model bias in terms of lower tropospheric wind circulation vertical structure of specific humidity and precipitable water contents. The magnitude of error for these parameters increases with forecast lead time in both GFS T574 and T382. In the GFS T382, a belt of large positive error of PWC is noticed over north east Arabian Sea and adjoining western parts of the country, which is unlike GFS T574. Otherwise, the mean errors of PWC over most parts of the country are negative in both GFS T574 and T382, which is found to be broadly in well agreement with the corresponding mean error (underestimation) pattern of rainfall over the country. Zonally averaged specific humidity shows that in the lower troposphere below 550 hPa between lat 10°N and 15°N, there is a negative bias of specific humidity. Above 550 hPa, the error is positive with a maximum value between 600 and 500 hPa and lat 10°N–15°N. GFS T382 shows negative bias below 850 hPa with a minimum value at 950 hPa between lat 5°N–10°N hPa and a strong positive bias above 850 hPa with a large domain of maximum value at 700 hPa between lat 5°N–10°N. GFS T574 forecast shows bias of westerly wind over most part of central and north India extending up to foot hills of Himalaya, south-westerly bias over the north west India and northeast Arabian sea, and northerly bias over east coast of India and adjuring Bay of Bengal extending southwards up to 15°N at 850 hPa. GFS T382 shows strong south-westerly bias over northwest India and adjoining Pakistan, where PWC showed strong positive bias.

Case study of monsoon depression demonstrated the superiority of the GFS T574 to improve track forecasts, due to improved vortex relocation algorithm of the model. The distribution of rainfall and its spatial CC in association with this depression produced by GFS T574 suggest that the model forecast provides useful guidance for real time forecasting of heavy rainfall in association with monsoon depression.

Further improvement in the forecast is expected with the possible inclusion of three dimensional hybrid ensemble KnF (Hamill et al. 2011) data assimilation and multiple physics. The model would continue to play increasingly important role to deliver better forecast services to the society in short to medium range time scale.

Acknowledgments This study for the Indian region with the use of GFS was possible due to the Monsoon Mission Programme launched by Ministry of Earth Sciences (MoES), Government of India. Authors are grateful to MoES and Director General of Meteorology, India Meteorological Department for providing all facilities to carry out this research work. Acknowledgements are due to NCEP, USA for providing the source codes and support for the implementation of the upgraded Version GFS T574 at IMD. Authors acknowledge the use of TRMM Products of NASA, USA in this work.

References

- Belair S, Methot A, Mailhot J, Bilodeau B, Patoine A, Pellerin G, Cote J (2000) Operational implementation of the Fritsch-Chappell convective scheme in the 24-km Canadian regional model. *Weather Forecast* 15:257–274
- David FP, Derber JC (1992) The national meteorological center's spectral statistical-interpolation analysis system. *Mon Weather Rev* 120:1747–1763
- Doswell CA III, Davies-Jones R, Keller DL (1990) On summary measures of skill in rare event forecasting based on contingency tables. *Weather Forecast* 5:576–585
- Durai VR, Roy Bhowmik SK, Mukhopadhyaya B (2010a) Performance Evaluation of precipitation prediction skill of NCEP global forecasting system (GFS) over Indian region during Summer Monsoon 2008. *Mausam* 61(2):139–154
- Durai VR, Roy Bhowmik SK, Mukhopadhyaya B (2010b) Evaluation of Indian summer monsoon rainfall features using TRMM and KALPANA-1 satellite derived precipitation and rain gauge observation. *Mausam* 61(3):317–336
- Hamill TM, Whitaker JS, Fiorino M, Benjamin SG (2011) Global ensemble predictions of 2009's tropical cyclones initialized with an ensemble Kalman filter. *Mon Weather Rev* 139:668–688
- Han J, Pan H-L (2006) Sensitivity of hurricane intensity forecast to convective momentum transport parameterisation. *Mon Weather Rev* 134:664–674
- Han J, Pan H-L (2010) Revision of convection and vertical diffusion schemes in the NCEP global forecast system. NCEP Office Note 464, 42 pp. Available online at: <http://www.emc.ncep.noaa.gov/officenotes/newernotes/on464.pdf>
- Kalnay E, Kanamitsu M, Baker WE (1990) Global numerical weather prediction at the National Meteorological Center. *Bull Am Meteorol Soc* 71:1410–1428
- Kanamitsu M (1989) Description of the NMC global data assimilation and forecast system. *Weather Forecast* 4:335–342
- Kanamitsu M, Alpert JC, Campana KA, Caplan PM, Deaven DG, Iredell M, Katz B, Pan H-L, Sela J, White GH (1991) Recent changes implemented into the global forecast system at NMC. *Weather Forecast* 6:425–435
- Kleist DT, Parrish DF, Derber JC, Treadon R, Wu W-S, Lord S (2009) Introduction of the GSI into the NCEP global data assimilation system. *Weather Forecast* 24:1691–1705
- McBride JL, Ebert EE (2000) Verification of quantitative precipitation forecasts from operational numerical weather prediction models over Australia. *Weather Forecast* 15:103–121
- Mlawer EJ, Taubman SJ, Brown PD, Iacono MJ, Clough SA (1997) Radiative transfer for inhomogeneous atmospheres: RRTM, a validated correlated-k model for the longwave. *J Geophys Res* 102:16663–16682
- Moorthi S, Pan HL, Caplan P (2001) Changes to the 2001 NCEP operational MRF/AVN global analysis/forecast system. NWS Technical Procedures Bulletin, 484, p 14. Available at <http://www.nws.noaa.gov/om/tpb/484.htm>
- Rajeevan M, Kale JD, Bhate J (2005) High-resolution gridded daily rainfall data for Indian monsoon studies, Tech. Rep. 2, National Weather Service, Pune, India
- Schaefer JT (1990) The critical success index as an indicator of warning skill. *Weather Forecast* 5:570–575
- Schultz P (1995) An explicit cloud physics parameterization for operational numerical weather prediction. *Mon Weather Rev* 123:3331–3343
- Saha S et al (2010) The NCEP climate forecast system reanalysis. *Bull Am Meteorol Soc* 91:1015–1057. doi:[10.1175/2010BAMS3001.1](https://doi.org/10.1175/2010BAMS3001.1)
- Saulo AC, Seluchi M, Campetella C, Ferreira L (2001) Error Evaluation of NCEP and LAHM Regional Model Daily Forecasts over Southern South America. *Weather Forecast* 16: 697–712
- Wang W, Seaman NL (1997) A comparison study of convective parameterization schemes in a mesoscale model. *Mon Weather Rev* 125:252–278
- Yang F, Pan H-L, Krueger SK, Moorthi S, Lord SJ (2006) Evaluation of the NCEP global forecast system at the ARM SGP site. *Mon Weather Rev* 134:3668–3690. doi:[10.1175/MWR3264.1](https://doi.org/10.1175/MWR3264.1)
- Yang F, Mitchell K, Hou Y-T, Dai Y, Zeng X, Wang Z, Liang X-Z (2008) Dependence of land surface albedo on solar zenith angle: observations and model parameterization. *J Appl Meteorol Climatol* 47:2963–2982. doi:[10.1175/2008JAMC1843.1](https://doi.org/10.1175/2008JAMC1843.1)